CIT - ELECTRON TUBE & MICROWAVE LABORATORY REPORT

Resonance Cones in the Field Pattern of a Short Radio Frequency Probe in a Warm Anisotropic Plasma

R. K. Fisher

Technical Report

CALIFORNIA INSTITUTE OF TECHNOLOGY

PASADENA, CALIFORNIA

RESONANCE CONES IN THE FIELD PATTERN OF A SHORT RADIO FREQUENCY PROBE IN A WARM ANISOTROPIC PLASMA

Thesis by

Raymond Kurt Fisher

In Partial Fulfillment of the Requirements

For the Degree of

Doctor of Philosophy

California Institute of Technology

Pasadena, California

1970

(Submitted March 16, 1970)

ACKNOWLEDGMENTS

The author wishes to express his deep appreciation to his advisor, Professor Roy W. Gould, for his suggestion of the problem and his continued guidance, encouragement and constant interest throughout the course of this research. His many direct contributions to this work are gratefully acknowledged.

The author is also indebted to Mr. Nagendra Singh for his work on some of the theoretical aspects of this research. Many members of the Plasma Laboratory contributed directly or indirectly to this work, and particular thanks go to Mr. James Downward for many helpful discussions and for the use of his apparatus during the initial stages of this research, Dr. Reiner Stenzel and Professor Robert S. Harp for their very helpful comments and advice, and Mr. Charles Moeller for his help in the microwave interferometer measurements. Special thanks are extended to Mrs. Ruth Stratton for her excellent typing of the manuscript. The author gratefully acknowledges the generous financial support he received from the National Science Foundation during the course of his graduate work. This investigation was supported in part by the United States Office of Naval Research and in part by the United States Atomic Energy Commission.

This work is dedicated to the author's wife, Sally, whose love, patience, encouragement and understanding have been helpful in many ways.

ABSTRACT

An experimental investigation of the angular field pattern of a small radio frequency probe in a plasma in a magnetic field is described. The field is observed to become very large along a resonance cone whose axis is parallel to the static magnetic field and whose opening angle is observed to vary with incident probe frequency, electron cyclotron frequency, and electron plasma frequency in agreement with simple cold plasma dielectric theory. The use of the resonance cone angle as a diagnostic tool to measure the plasma density in a plasma in a magnetic field is discussed. It is noted that similar cones might be expected near the ion cyclotron frequency.

The relationship of these cones to the limiting phase- and group-velocity cones which appear in the theory of plane wave propagation is discussed. The necessity for examining the allowed directions of the group velocity rather than the allowed directions of the phase velocity and customary phase velocity plots when determining whether propagation between two remote points in a plasma is possible, is emphasized.

The addition of electron thermal velocities to the theory is examined in the limit of a large static magnetic field. The resonance cone angle is shifted to a slightly smaller angle than that predicted by cold plasma theory, and a fine structure appears inside the cones and is shown to result from an interference between a fast electromagnetic wave and a slow plasma wave. The interference structure is observed experimentally, and measurements of the angular intereference spacing are shown to agree with the warm plasma theory.

TABLE OF CONTENTS

I. INTRODUCTION

The electromagnetic fields and radiation from sources in a plasma in a magnetic field have been the subject of many theoretical studies and have become of practical interest in connection with investigations employing rocket and satellite vehicles.

Much of the theoretical work has centered on the small dipole antenna. F. Bunkin [1] was the first to study the radiation fields of an electric dipole in an anisotropic medium. H. Kogelnik [2,3] investigated the radiation resistance of a point electric dipole in an anisotropic plasma. H. Kuehl [4,5] found expressions for the far-zone electric field of an electric dipole in a cold anisotropic plasma and pointed out the existence of a singularity in the angular field pattern. His analysis of an oscillating point dipole showed that the fields should become infinite along a cone whose axis is parallel to the static magnetic field and whose opening angle is determined by the plasma density, magnetic field strength and incident frequency (see Fig. 1.1). T. Kaiser [6] was also one of the first authors to discuss this singularity, which will be referred to as the resonance cones.

At the Symposium on Electromagnetic Theory and Antennas held in Copenhagen, Denmark in 1962, several important papers on the subject under discussion were presented. E. Arbel and L. Felsen [7,8] discussed radiation from sources in anisotropic media with particular attention to the singularity in the fields on the resonance cones. P. Clemmow [9,10] introduced a simple scaling procedure which he used to obtain the dipole fields and the resonance cones. H. Motz and H. Kogelnik [11]

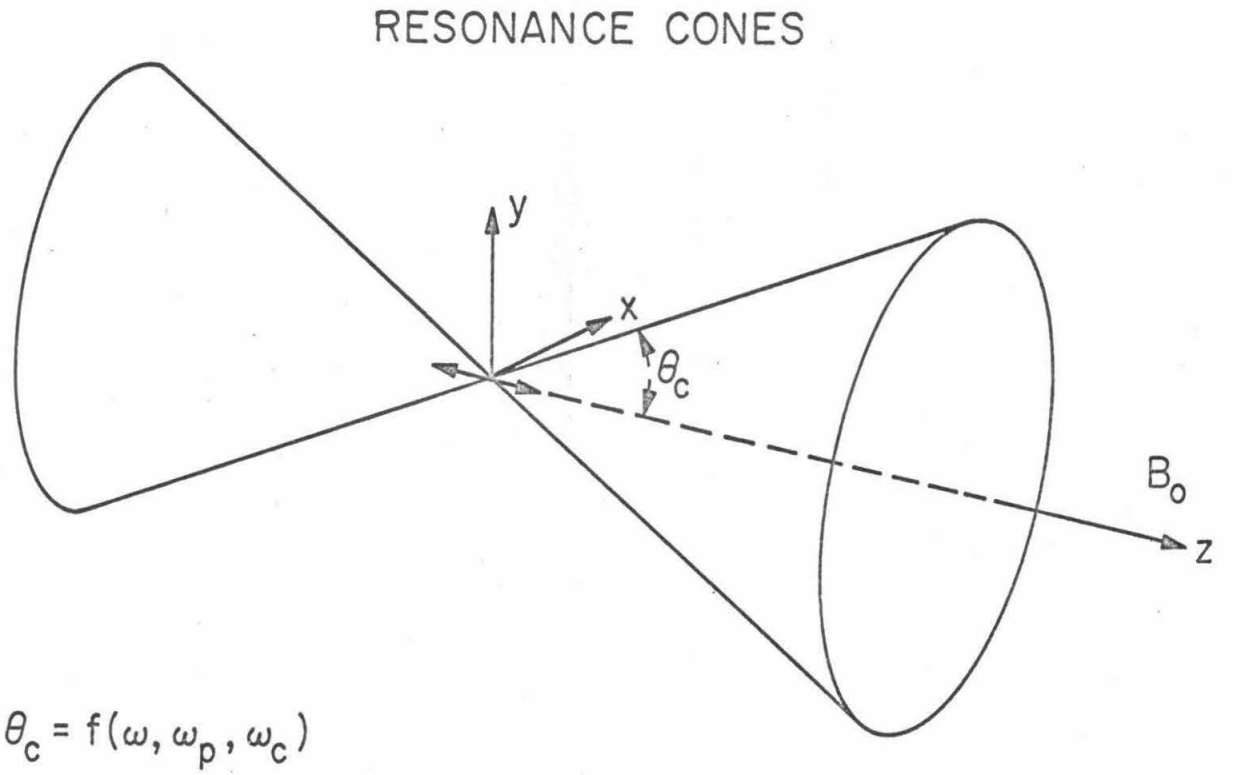

Fig. 1.1 Diagram showing resonance cones for a small antenna located at the origin. The axis of the cones is parallel to the static magnetic field B_o and the opening angle θ_c is determined by the plasma frequency ω_p, cyclotron frequency ω_c, and incident frequency ω.

discussed radiation from sources embedded in an anisotropic medium and showed that the time-average Poynting vector is parallel to the group velocity. R. Mittra and G. Deschamps [12] solved for the fields at an arbitrary distance from the dipole, including the near-zone fields.

The singularity at the resonance cone in the fields of a point dipole has stirred considerable controversy. Kuehl's analysis of the far fields [4,5] shows that the Poynting vector is also singular on the resonance cones, so that the total power flow and hence the radiation resistance is infinite for the point dipole antenna. This result, sometimes referred to as the "infinity catastrophe", has caused K. Lee and C. Papas [13] to introduce a new theory for the calculation of the radiation resistance of antennas in anisotropic media, using only the portion of the total time-average power which is time-irreversible. This has been critized by H. Staras [14] who argues that the singularity arises not from the method of calculation, but rather from a physical inconsistency in the Appleton-Hartree dielectric tensor; and by D. Walsh and H. Weil [15] who point out apparent difficulties in the Lee and Papas method. Lee and Papas have written further papers in defense of their theory [16,17].

The inclusion of effects such as electron collisions, electron thermal velocities, and sources of non-zero dimensions have been shown to cause the fields along the cones (and hence the radiation resistance) to remain finite. Arbel and Felsen [8] and Staras [18] have shown that the singularity vanishes for a source distribution of finite extent. Kaiser [6] has shown that the inclusion of electron collisions results in finite fields on the resonance cones. In a very recent paper,

N. Singh and R. Gould [19] have shown that the addition of electron thermal velocities also eliminates the singularity. G. Deschamps and O. Kesler [20] also discuss the resonance cones in a warm magnetoplasma. J. Tunaley and R. Grard [21] have discussed the suppression of the singularity through the interaction of the thermal electrons with the probe fields.

S. Lee and R. Mittra [22] have discussed the singularity on the resonance cones in solving for the transient radiation of an electric dipole in a uniaxial plasma, and suggest the need for a more realistic model including finite losses. J. Kenny [23] has also studied the transient problem and has pointed out an essential error made in the calculations of Lee and Mittra.

Quasistatic methods have been employed by B. Kononov, et al [24], Kaiser [6], and K. Balmain [25] to investigate the near fields of a short dipole antenna in a magnetoplasma. Kaiser and Balmain use these fields to calculate the antenna impedance. T. Wang and T. Bell [26] have shown agreement between a full electromagnetic treatment and the quasistatic solutions for the impedance. Balmain suggests that in a lossy plasma the high-level near fields on the resonance cones extend outward to a distance comparable to the dimension of the source divided by the relative collision frequency.

Considering the extent of the theoretical work on radiation from sources in anisotropic plasmas and the interest shown in the resonance cones, there has been remarkably little experimental activity in these areas. Balmain [25] has done some antenna impedance measurements in a magnetoplasma. Kononov, et al [24] have investigated the resonance at

$\theta = 0^{o}$ (along the field) for $\omega = (\omega_c^2 + \omega_p^2)^{1/2}$. The data from the Alouette satellite has inspired considerable work on the cyclotron harmonics and propagation across the field ($\theta = 90^{o}$) [27]. This thesis describes an investigation of the angular field pattern of a small rf probe in a plasma in a magnetic field and represents the first experimental verification of the existence of resonance cones along which the observed fields become very large.

Chapter II is devoted to theory. The quasistatic potential of an oscillating charge in a uniform cold plasma in a magnetic field is calculated and shown to exhibit the resonance cones. The resonance cones are shown to exist regardless of the charge distribution on the exciting probe. The connection between the quasistatic solution for the probe fields and the far-field electromagnetic solution is discussed.

In Chapter III the experimental apparatus and procedures are described. Details of the plasma generation, operating conditions, and magnetic field configuration are given. The geometry and construction of the transmitting and receiving probes used to measure the resonance cones are discussed. The details of the experimental electronics for measurements of both the amplitude and phase of the received signal are given.

In Chapter IV measurements of the experimental resonance cone angle as a function of the probe frequency and cyclotron frequency are presented and are shown to agree with the cold plasma dielectric theory for a given plasma frequency. An independent measurement of the plasma density using a microwave interferometer confirms this value for the

plasma frequency. Measurements of the cone angle at different radii show that the radial density profile in the plasma column is relatively uniform out to the maximum probe separation used in the experiment. The use of the resonance cone angle as a diagnostic tool to measure the plasma density in a plasma in a magnetic field is discussed. Measurements of the phase of the received signal are discussed in an attempt to determine the multipolar nature of the probe fields.

Chapter V discusses the relationship of these cones to the limiting phase- and group-velocity cones which appear in the theory of plane wave propagation. The index of refraction and wave vector $\underline{k}$ for the propagation of plane waves in a magnetoplasma become singular at certain angles with respect to the static magnetic field direction, and this angle is sometimes also referred to as the resonance cone angle. This resonance angle is the complementary angle of the angle at which the fields of a small source in a magnetoplasma become singular, and the difference is explained in terms of the directions of the phase and group velocities in an anisotropic plasma. The necessity for examining the allowed directions of the group-velocity rather than the allowed directions of the phase-velocity and the customary phase velocity plots, when determining whether propagation between two remote points in a plasma is possible, is emphasized.

Chapter VI discusses warm plasma effects on the structure of the resonance cones. In the limit of a large static magnetic field ($\omega_c >> \omega_p, \omega$), the addition of electron thermal velocities is shown to modify the theory so that the cone angle is shifted to a slightly smaller angle than that predicted for the cold plasma, and an

interference structure appears inside the cone. This structure is shown to result from an interference between a fast electromagnetic wave and a slow plasma wave. The interference structure is observed experimentally and the electron temperature inferred from a comparison of the experimental angular spacing between two adjacent maxima in the interference structure to that calculated theoretically is in agreement with an independent Langmuir probe temperature measurement. The experimental interference spacing is also shown to vary with the probe separation in agreement with theory.

The results and conclusions are summarized in Chapter VII and some suggestions for further work are given. The observations of the resonance cones were first reported in May 1969 in Physical Review Letters (Appendix A). The warm plasma results have been submitted for publication in Physics Letters. The relationship of these cones to the limiting phase- and group-velocity cones which appear in the theory of plane wave propagation was first discussed at the Ninth International Conference on Phenomena in Ionized Gases, Bucharest, Romania, Sept. 1969 and appears in the published proceedings of that conference (Appendix E).

II. THEORY FOR A COLD PLASMA

Consider a probe oscillating at frequency ω in an infinite homogeneous collisionless plasma with an applied static magnetic field $\underline{B}_o = B_o \hat{z}$. The near-zone fields ($r << c/\omega$) may be derived using the quasistatic approximation $\underline{E} = -\nabla\emptyset$. We must solve Poisson's equation:

$$\nabla \cdot \underline{D} = \rho_{ext} \tag{2.1}$$

where ρ_{ext} is the charge distribution on the probe. For a plasma in a magnetic field:

$$\underline{D} = \varepsilon_o \underline{\underline{K}} \cdot \underline{E} \tag{2.2}$$

where $\underline{\underline{K}}$ is the dielectric tensor of form

$$\underline{\underline{K}} = \begin{pmatrix} K_\perp & -K_H & 0 \\ K_H & K_\perp & 0 \\ 0 & 0 & K_\parallel \end{pmatrix} \tag{2.3}$$

in Cartesian coordinates. For a cold plasma, neglecting terms of order m_e/m_i ,

$$K_\perp = 1 - \frac{\omega_p^2}{\omega^2 - \omega_c^2} \quad ; \quad K_H = \frac{i\omega_p^2 \omega_c}{(\omega^2 - \omega_c^2)} \quad ;$$

$$\text{and} \qquad K_\parallel = 1 - \frac{\omega_p^2}{\omega^2} \tag{2.4}$$

These expressions are valid for frequencies ω large compared to Ω_p and Ω_c, the ion plasma and ion cyclotron frequencies. For simplicity

we will solve for the potential of an oscillating monopole located at the origin

$$\rho_{ext} = qe^{-i\omega t}\,\delta(\underline{r}) \tag{2.5}$$

Although this is a non-physical charge distribution, the solution we will obtain with $q = 1$ can be thought of as the Green's function for the problem and will therefore be useful.

The coordinate system is shown below:

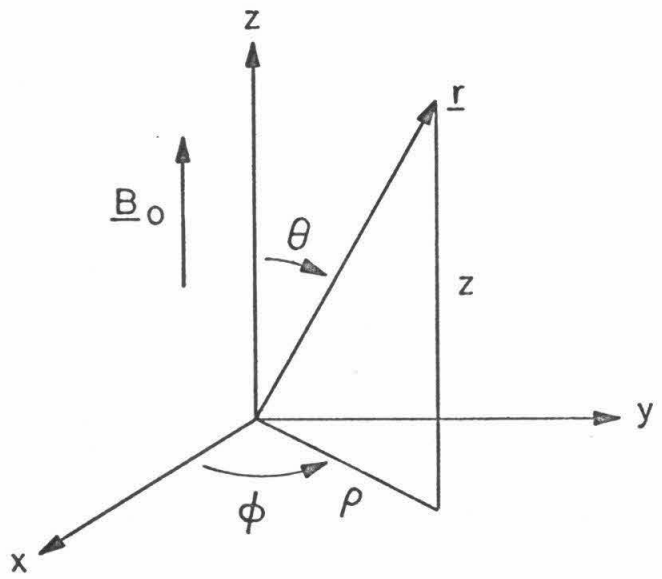

Poisson's equation becomes

$$-\nabla \cdot \underline{\underline{K}} \cdot \nabla\emptyset = qe^{-i\omega t}\,\delta(\underline{r})/\varepsilon_o \tag{2.6}$$

Taking the Fourier transform of this equation

$$\underline{k} \cdot \underline{\underline{K}} \cdot \underline{k}\,\Phi_k = qe^{-i\omega t}/\varepsilon_o \tag{2.7}$$

so that

$$\phi = \frac{qe^{-i\omega t}}{\varepsilon_o} \iiint \frac{e^{i\underline{k}\cdot\underline{r}}}{k_\perp^2 K_\perp + k_\parallel^2 K_\parallel} \frac{d^3\underline{k}}{(2\pi)^3} \tag{2.8}$$

Let $\underline{r} = (\rho,0,z)$ in cylindrical coordinates and $\underline{k} = (k_\perp \sin\phi, k_\perp \cos\phi, k_\parallel)$ so that:

$$\phi(\rho,0,z) = \frac{qe^{-i\omega t}}{4\pi^2 \varepsilon_o} \int_{-\infty}^{\infty}\int_0^{\infty} \frac{e^{ik_\parallel z} k_\perp dk_\perp dk_\parallel}{(k_\perp^2 K_\perp + k_\parallel^2 K_\parallel)} \int_0^{2\pi} e^{ik_\perp \rho \sin\phi} \frac{d\phi}{2\pi} \tag{2.9}$$

Performing the integration over ϕ yields

$$\phi(\rho,0,z) = \frac{qe^{-i\omega t}}{4\pi^2 \varepsilon_o} \int_{-\infty}^{\infty} e^{ik_\parallel z} dk_\parallel \int_0^{\infty} \frac{J_o(k_\perp \rho)}{k_\perp^2 K_\perp + k_\parallel^2 K_\parallel} k_\perp dk_\perp \tag{2.10}$$

(see Gradshteyn and Ryzhik, Tables of Integrals, Series and Products, integral 8.411-1, p. 952.) Since the integrand in the integral over $k_\perp$ is an even function of $k_\parallel$

$$\phi(\rho,0,z) = \frac{qe^{-i\omega t}}{2\pi^2 \varepsilon_o} \int_0^{\infty} \cos k_\parallel z \, dk_\parallel \int_0^{\infty} \frac{J_o(k_\perp \rho)}{k_\perp^2 K_\perp + k_\parallel^2 K_\parallel} k_\perp dk_\perp \tag{2.11}$$

Now performing the integration over $k_\perp$, we have

$$\phi(\rho,0,z) = \frac{qe^{-i\omega t}}{2\pi^2 \varepsilon_o K_\perp} \int_0^{\infty} K_o[k_\parallel (K_\parallel / K_\perp)^{1/2} \rho] \cos k_\parallel z \, dk_\parallel \tag{2.12}$$

(see Gradshteyn and Ryzhik, integral 6.532-4, p. 678.) Here K_o is the modified Bessel function. For $K_\parallel / K_\perp < 0$, equation (2.12) can be rewritten

$$\phi(\rho,z) = \frac{qe^{-i\omega t}}{2\pi^2\varepsilon_o K_\perp} \int_0^\infty \frac{i\pi}{2} H_o^{(1)} [k_\parallel \alpha\rho] \cos k_\parallel z \, dk_\parallel \qquad (2.13)$$

where $H_o^{(1)}$ is the Hankel function of the first kind, and $\alpha = (-K_\parallel / K_\perp)^{1/2} > 0$. Thus

$$\phi(\rho,z) = \frac{iqe^{-i\omega t}}{4\pi\varepsilon_o K_\perp} \int_0^\infty [J_o(k_\parallel \alpha\rho) + iN_o(k_\parallel \alpha\rho)] \cos k_\parallel z \, dk_\parallel \qquad (2.14)$$

$$= \frac{iqe^{-i\omega t}}{4\pi\varepsilon_o K_\perp} \left[\left\{ \begin{array}{c} \frac{1}{(\alpha^2\rho^2 - z^2)^{1/2}} \\ 0 \end{array} \right\} + i \left\{ \begin{array}{c} 0 \\ \frac{-1}{(z^2 - \alpha^2\rho^2)^{1/2}} \end{array} \right\} \right] \quad \text{for} \quad \begin{array}{l} \alpha\rho > z \\ \alpha\rho < z \end{array} \qquad (2.15)$$

(see Gradshteyn and Ryzhik, integrals 6.671-8 and 6.671-12, p. 731.), so that

$$\phi(\rho,z) = \frac{qe^{-i\omega t}}{4\pi\varepsilon_o (K_\perp^2 K_\parallel)^{1/2} [(\rho^2/K_\perp) + (z^2/K_\parallel)]^{1/2}} \qquad (2.16)$$

For $K_\parallel / K_\perp > 0$ equation (2.16) follows directly from (2.12), (see Gradshteyn and Ryzhik, integral 6.671-14, p. 732.) Equation (2.16) is very similar to the potential of an oscillating charge in free space except that the coordinates ρ,z are scaled by the appropriate dielectric constant in that coordinate direction.

To solve for the potential and fields of an oscillating dipole we merely take the appropriate derivatives. All spatial derivatives of Eq. (2.16), however, will also have a singularity along the cone defined by the vanishing of the denominator

$$K_{\parallel} \sin^2\theta + K_{\perp} \cos^2\theta = 0 \qquad (2.17)$$

where $\theta = \tan^{-1}\rho/z$ is the polar angle in spherical coordinates. As pointed out previously, the potential (2.16) with $q = 1$ can be thought of as the Green's function for the problem and thus the resonance cones will exist regardless of the charge distribution on the exciting probe. The cones exist only in the frequency regions where either $K_{\perp}$ or $K_{\parallel}$ becomes negative, but not both. Equation (2.17) can be rewritten

$$\tan^2\theta_c = -K_{\perp}/K_{\parallel} \qquad (2.18)$$

Figure 2.1 shows the ratio $K_{\perp}/K_{\parallel}$ plotted versus ω, the probe frequency. There are two frequency regions or "branches" where $K_{\perp}/K_{\parallel} < 0$ and cones exist. For ω less than both ω_p and ω_c, $K_{\perp} > 0$ and $K_{\parallel} < 0$. This region will be called the "lower branch". No cones will exist for ω between ω_p and ω_c. Again there will be cones for ω greater than both ω_p and ω_c but less than $\omega_{uh} = (\omega_p + \omega_c)^{1/2}$, the electron upper hybrid frequency, for then $K_{\perp} < 0$ and $K_{\parallel} > 0$. This region will be designated as the "upper branch". No cones will exist for $\omega > (\omega_c + \omega_p)^{1/2}$. We can see that in the lower branch, as ω increases the ratio $-K_{\perp}/K_{\parallel}$ increases, and hence θ_c increases, while in the upper branch as ω increases, θ_c decreases.

Substituting equations (2.4) into (2.18), we can solve for

$$\sin^2\theta_c = \frac{\omega^2(\omega_p^2 + \omega_c^2 - \omega^2)}{\omega_p^2\,\omega_c^2} \qquad (2.19)$$

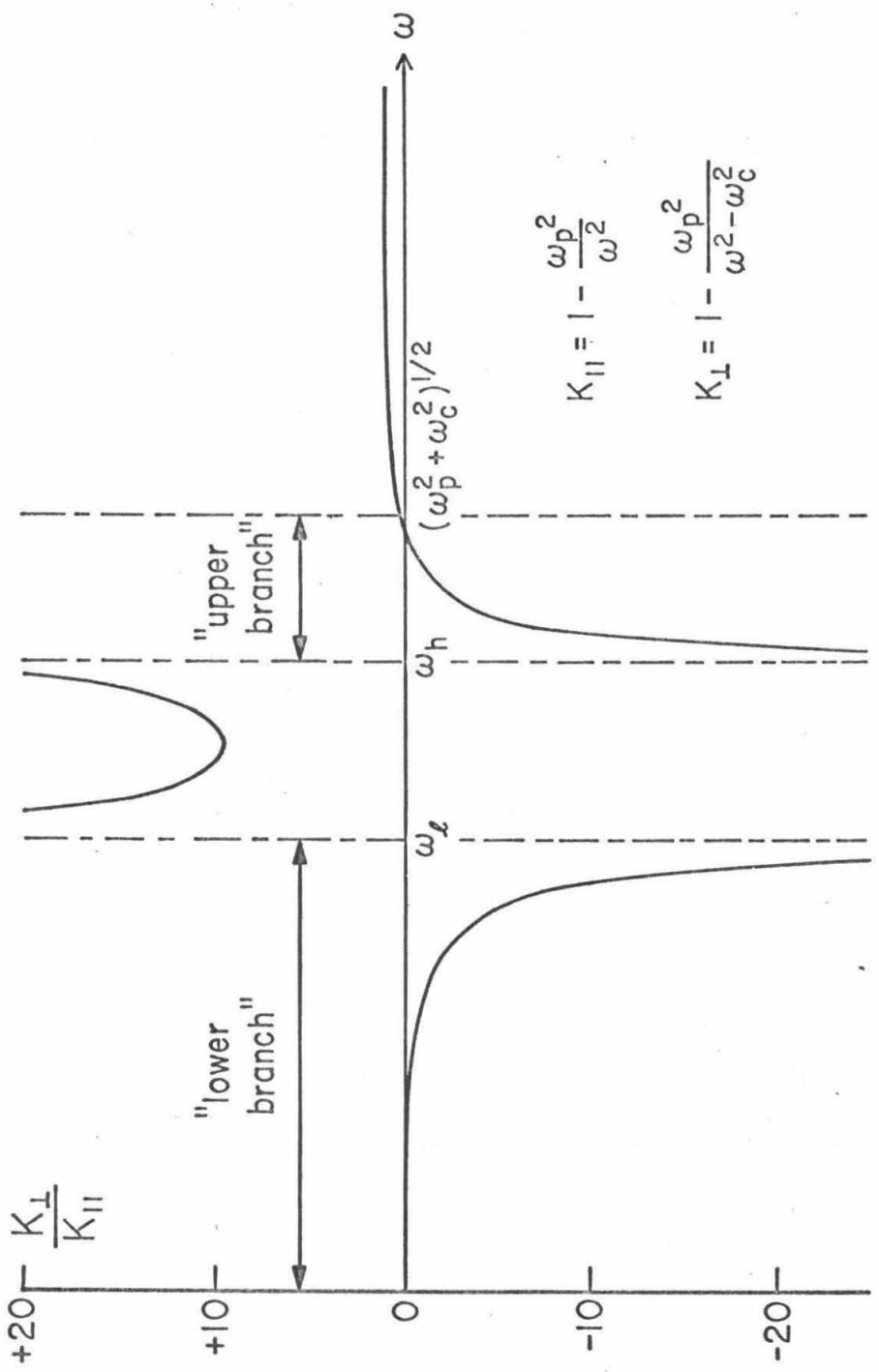

Fig. 2.1 $K_\perp/K_{||}$ versus incident probe frequency. Cones exist only where $K_\perp/K_{||} < 0$, and these frequency regions are designated as the "lower branch" ($\omega < \omega_p, \omega_c$) and the "upper branch" ($\omega_p, \omega_c < \omega < (\omega_p + \omega_c)^{1/2}$). Here ω_ℓ and ω_h represent the lower and higher of the plasma and cyclotron frequencies.

which gives the cone angle as a function of the probe frequency, plasma frequency, and cyclotron frequency in the plasma. Note that it is symmetric with respect to ω_p and ω_c.

A calculation of the fields of an oscillating point dipole in an anisotropic plasma based on the full set of Maxwell's equations [5] shows that the fields should also become singular at this same cone angle in the far-zone region ($r >> c/\omega$). The validity of the quasistatic solution presented here is not simply that the near-zone condition ($r << c/\omega$) apply. We are dealing with a resonance ($n \to \infty$) where electrostatic approximations are usually valid. The quasistatic solutions for the electric field are valid near the resonance cone (see Appendix B).

It should be noted that similar cones might be expected near the ion cyclotron frequency. This can be seen in Fig. 2.2 where the ratio $K_\perp/K_\parallel$ is plotted versus frequency for a two-component plasma. The ion terms have been included in the expressions for the plasma dielectric constants

$$K_\parallel = 1 - \frac{\omega_p^2}{\omega^2} - \frac{\Omega_p^2}{\omega^2} \quad \text{and} \quad K_\perp = 1 - \frac{\omega_p^2}{\omega^2 - \omega_c^2} - \frac{\Omega_p^2}{\omega^2 - \Omega_c^2} \tag{2.20}$$

and the assumption that the ion frequencies Ω_p and Ω_c are small compared to ω_p and ω_c, which is usually true, has been employed. Cones should exist in the frequency region $\omega < \Omega_c$, which will be designated as the "ion branch". Only one branch is seen near the ion frequencies while there are still two branches associated with the electron frequencies. This is because the Ω_p^2/ω^2 term remains small

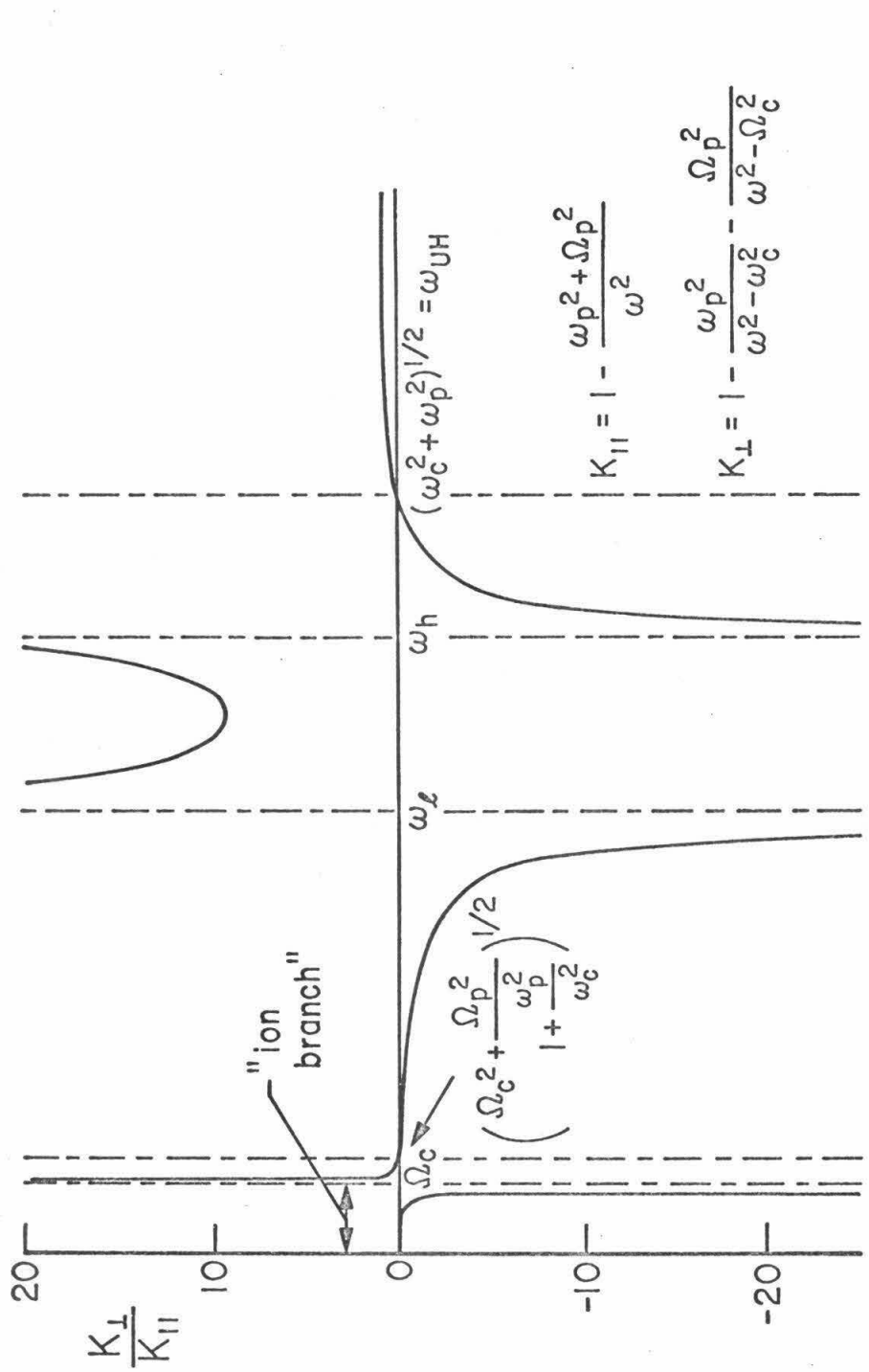

Fig. 2.2 $K_\perp/K_{11}$ versus incident probe frequency with ion terms included, leading to a new frequency region where cones should exist, the "ion branch" ($\omega < \Omega_c$). The assumption Ω_c, $\Omega_p << \omega_p, \omega_c$ which is usually true has been used here.

and has no significant effect on the sign of $K_{\parallel}$ but the $\Omega_p^2/(\omega^2 - \Omega_c^2)$ term becomes very large near Ω_c and so changes the sign of $K_{\perp}$. No attempt was made to experimentally observe these ion branch cones.

The resonance cones may be thought of as a shift of the plasma resonances with angle. Heald and Wharton [28] discuss the effect of the collective electron motion on the cyclotron resonance and obtain the equivalent of the upper branch of the cones. Akhiezer, et al [29] discuss the equivalent of the lower branch, upper branch, and ion branch as a shift in the frequency of the three longitudinal eigen-oscillations of a cold plasma in a magnetic field with angle. Note that the dielectric constants used in the quasistatic solution for the potential of an oscillating charge include the effects of the particle motion.

III. EXPERIMENTAL APPARATUS AND PROCEDURES

3.1 Plasma Generation and Confinement

The experiment was performed in a steady-state argon plasma, in the apparatus illustrated in Fig. 3.1.* The plasma was produced by gas-discharge breakdown in an rf electric field. The frequency (21 MHz) was chosen to be near the electron-neutral collision frequency, thus resulting in a low breakdown field strength.

The rf power was supplied by a 100W Johnson-Viking II transmitter coupled through a transmission line to a resonant circuit. Two cylindrical copper electrodes which fit tightly around the glass cylinder were connected to symmetric taps on the coil of the ungrounded resonant circuit.

The plasma was contained in a glass cylinder (Pyrex brand conical pipe, diameter $\simeq$ 15 cm). One end of the cylinder was connected to a standard high-vacuum station capable of producing a 10^{-6} to 10^{-7} Torr vacuum. An aluminum or glass plate sealed the other end of the glass cylinder.** Argon gas of research grade purity was introduced into the evacuated system through a variable leak valve. A small continuous flow (the valve between the diffusion pump and the system being almost closed) insured the highest possible purity of the gas involved in the plasma formation. The pressure was indicated by an ionization gauge located just above the diffusion pump.

---

*Neon was also used with essentially identical experimental results.

**The metallic end plate had no noticeable effect on the experimental results.

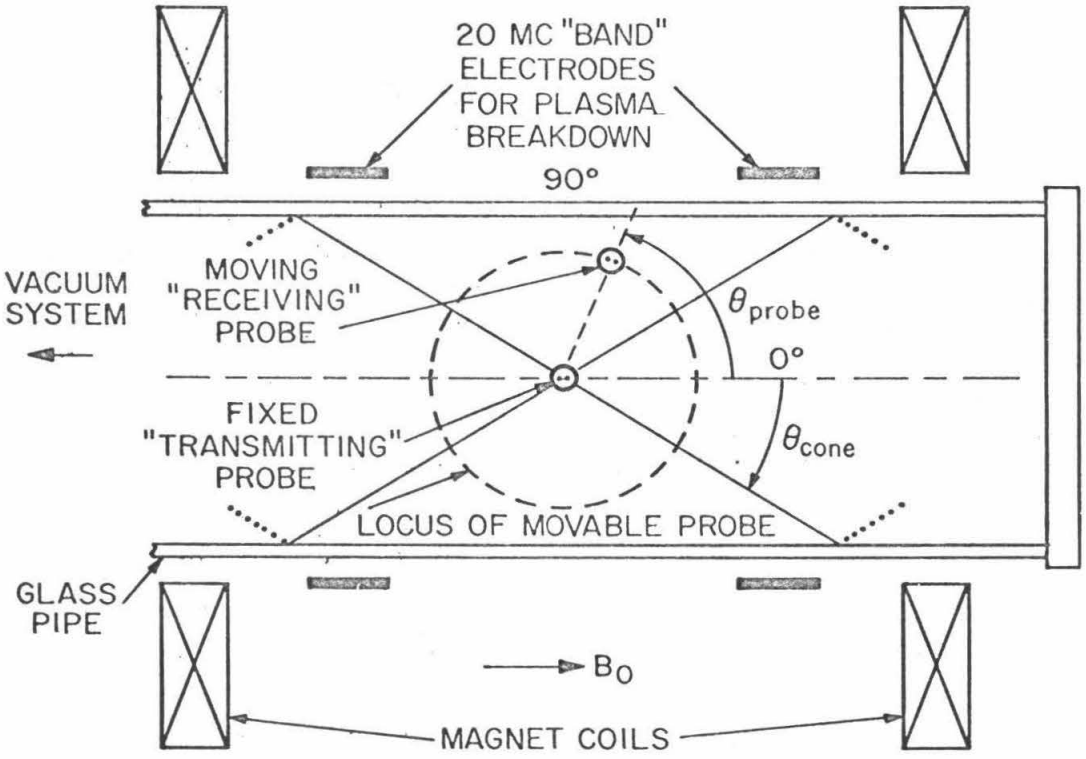

Fig. 3.1 Schematic of experiment to measure resonance cones

The active discharge region was about 25 cm long. In this region the electron density was approximately 10^{10} electrons/cm^3, corresponding to a plasma frequency $f_p = \omega_p/2\pi$ of about 900 MHz. The background neutral gas pressure was varied from 0.1 to 10 microns with most measurements done at approximately 1 micron.

A static magnetic field was produced along the axis of the plasma column by a pair of Helmholtz coils. The field strength could be varied from 0 to 600 gauss and was controlled by a current-regulated power supply. Thus the cyclotron frequency f_c could be varied from 0 to 1600 MHz. The field was calibrated using a rotating coil gaussmeter.

3.2 Transmitting and Receiving Probes

The transmitting and receiving probes used to study the resonance cones were introduced into the plasma through two ports on the opposite sides of the glass cylinder. The probes consisted of lengths of semi-rigid coaxial cable with about 2 mm of center conductor exposed. Probe construction is discussed in more detail in Appendix C. Referring again to Fig. 3.1, the transmitting probe was located at the center of the plasma column. A second probe was used to measure the fields set up by the transmitting probe. This receiving probe was constructed to rotate in a circular arc whose center is at the transmitting probe. If the incident frequency of the transmitting probe is chosen to be in a frequency range where cones exist, one would expect to see an increase in the received signal as the angle θ_p which the receiving probe position makes with respect to the magnetic field passes through the angle θ_c of the resonance cones set up by the transmitting probe.

3.3 Experimental Electronics

A block diagram of the experimental electronics is shown in Fig. 3.2. The signal into the transmitting probe was provided by a variable frequency UHF oscillator (various General Radio unit-oscillators in the 50-1800 MHz range). The signal from the receiving probe was mixed with a local oscillator signal and fed into a 30 MHz I-F amplifier (General Radio Type 1236 with General Radio Type 874-MRAL mixer). A band reject filter was inserted before the mixer to reduce the 21 MHz signal and its first harmonic present in the plasma. The I-F output was rectified by a crystal diode and drove the Y-axis of an X-Y recorder. The X-axis of the recorder was controlled by a potentiometer which measured the angular position of the receiving probe with respect to the direction of the static magnetic field.

To measure the relative phase of the received signal, and also to make more quantitative measurements of the resonance cone amplitude, a second detection system, shown in Fig. 3.3, was employed. Here the received signal was fed into the test channel of a Hewlett-Packard 8410A network analyzer with a 8413A phase-gain indicator plug-in module. A directional coupler connected to the signal source provided the input to the reference channel. The HP 8410A measured the amplitude and phase of the test channel relative to the reference channel and was equipped with output jacks so that either the amplitude (in db) or the phase (in degrees) could be used to drive the Y-axis of the X-Y recorder. Again the X-axis measured the receiving probe position with respect to the magnetic field direction.

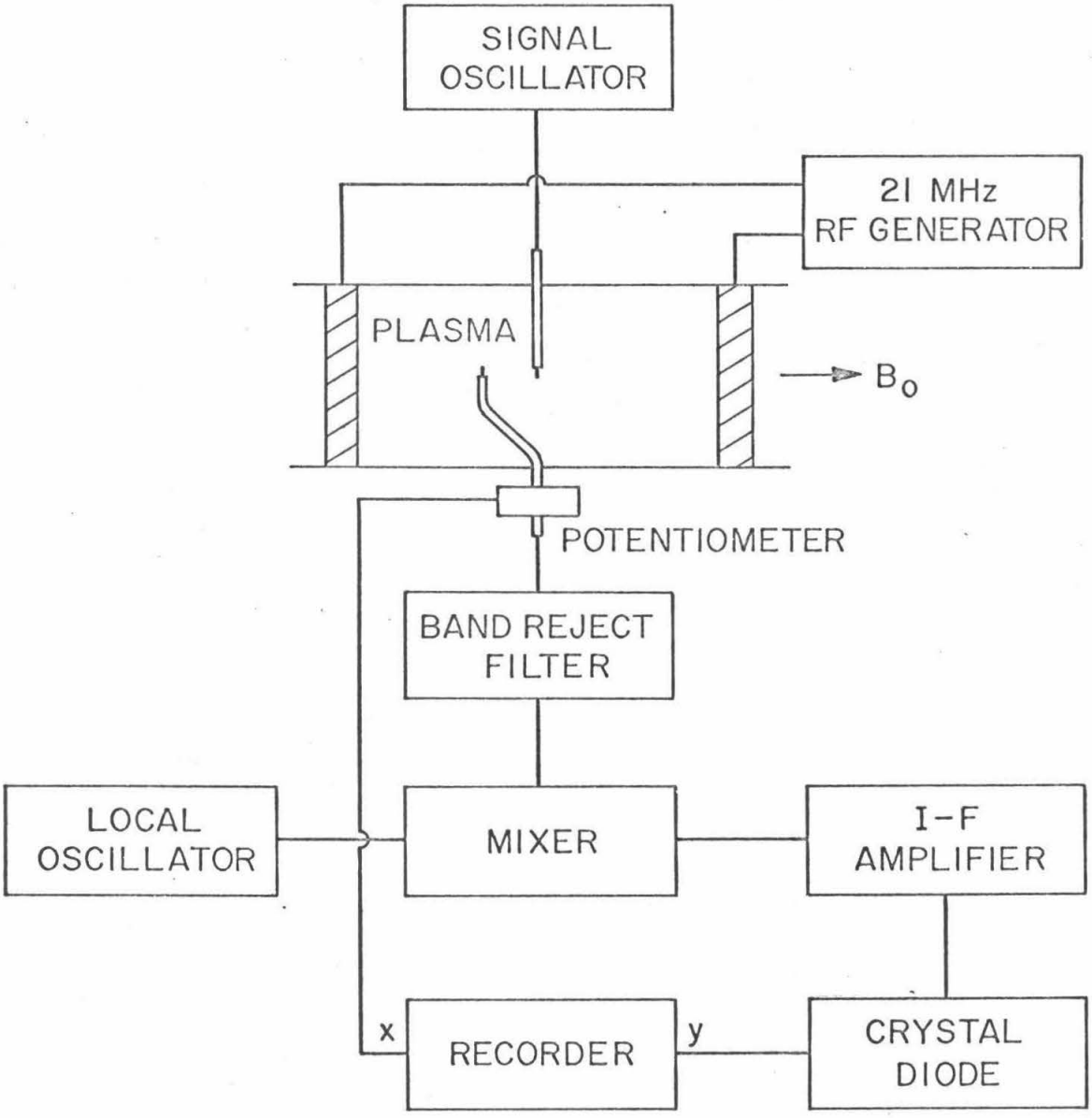

Fig. 3.2 Block diagram of experimental electronics

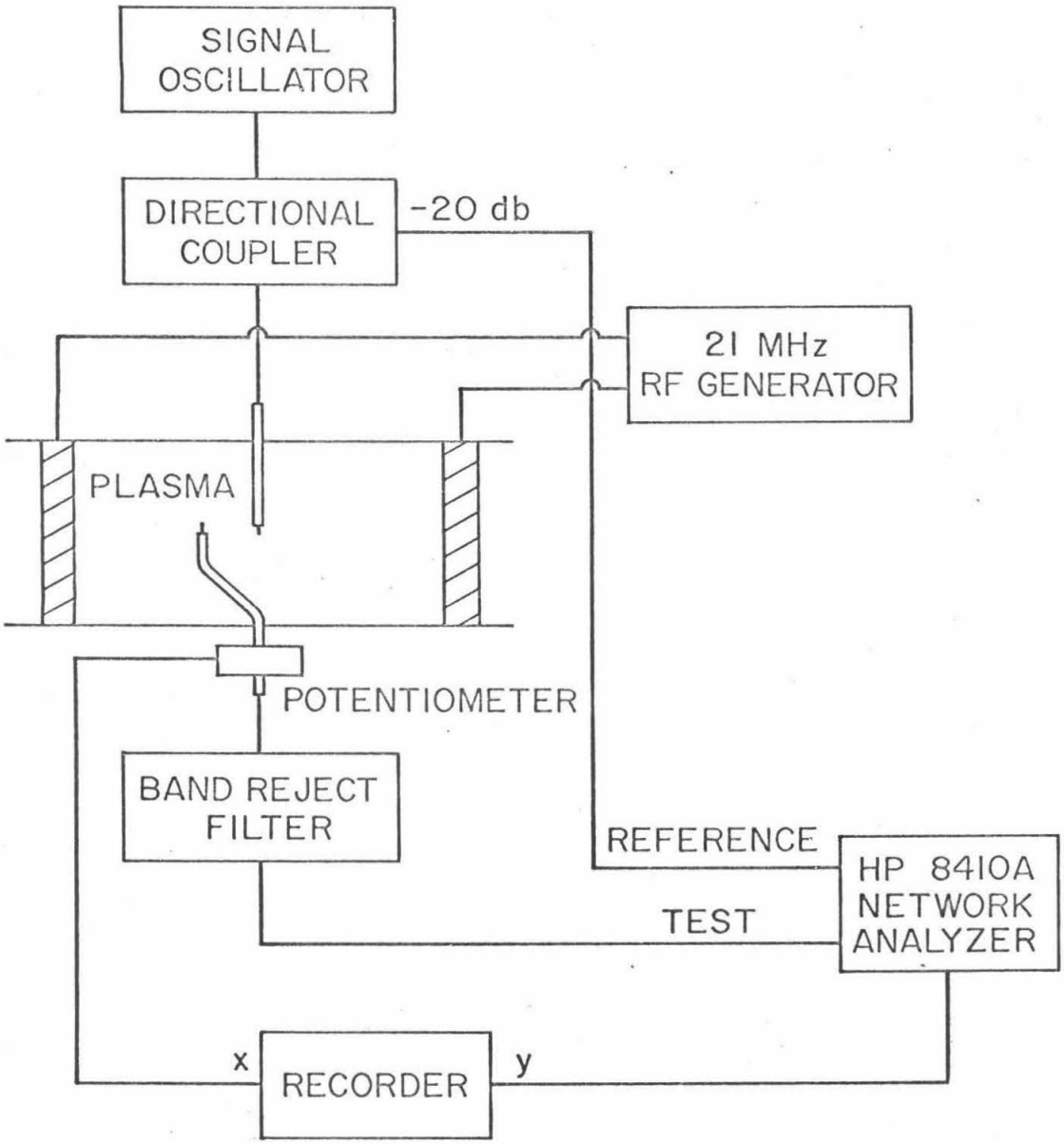

Fig. 3.3 Block diagram of experimental electronics when measuring amplitude and phase of received signal.

IV. EXPERIMENTAL RESULTS AND DISCUSSION

4.1 Amplitude Measurements and Cone Angle Location

The incident probe frequency f, plasma frequency f_p, and cyclotron frequency f_c were held constant and the angular field pattern of the transmitting probe was measured. A portion of a typical X-Y recorder trace is shown in Fig. 4.1. The vertical axis is the received signal from the I-F amplifier and the horizontal axis is θ_{probe}, the angle the position of the receiving probe makes with respect to the magnetic field direction. The received signal is observed to become very large at the resonance cone angle. The structure which appears just inside the cones will be discussed in Section VI.

When the cone angle exceeded about 60^o, additional broad peaks were seen in the field pattern inside the resonance cone angle. These are believed due to multiple reflections from the glass walls (dotted lines in Fig. 3.1). An angle of about 60^o is consistent with the time the reflected cone would first intersect the path of the receiving probe, given the geometry of the experiment. Also, experimentally these reflected peaks seem to be symmetric about $\theta = 0^o$ and both increase in number and move rapidly away from $\theta = 0^o$ as θ_c is increased. These observations are consistent with considerations of reflections from the walls.

In Fig. 4.2, the plasma density and magnetic field strength were held constant and traces were taken at various incident frequencies. It is seen that as the frequency was increased from 275 to 450 MHz, the resonance cone angle increased from about 25^o to about 45^o. This is

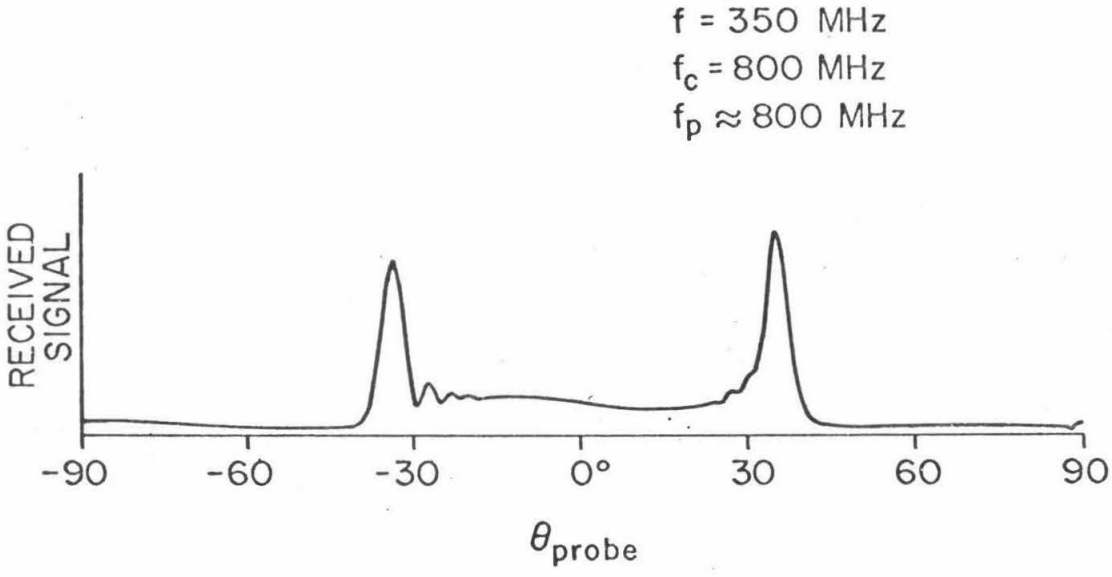

Fig. 4.1 Portion of a typical experimental trace showing the signal received by the rotating probe versus the angle the receiving probe makes with the magnetic field direction.

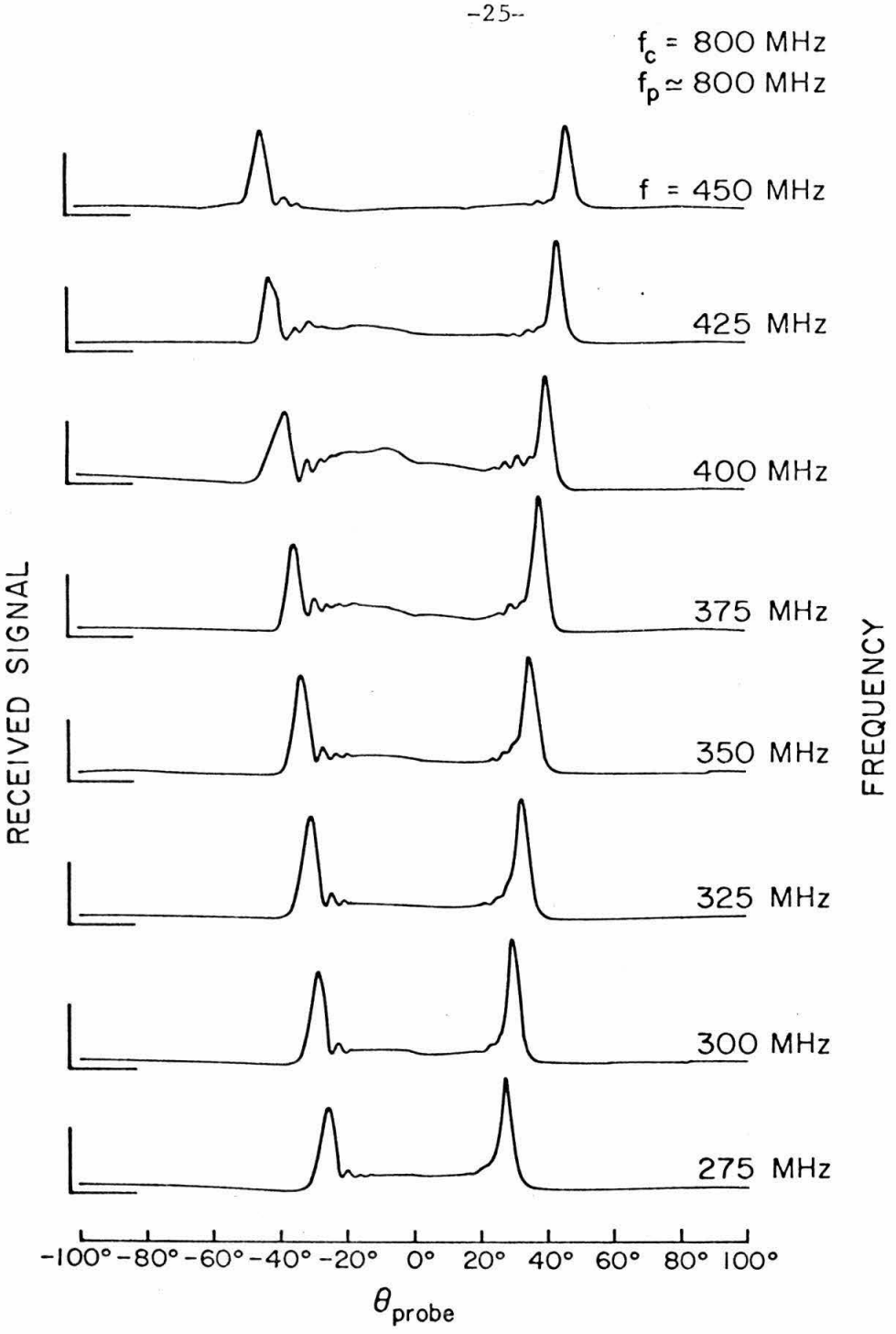

Fig. 4.2 Series of experimental traces showing variation of resonance cone angle with probe frequency for constant plasma density and constant magnetic field strength.

part of the lower branch since, as the frequency was increased, the cone angle increased.

If the experimentally measured cone angle is plotted versus the ratio ω/ω_c we obtain a measure of the plasma density as shown in Fig. 4.3. The solid curves are plots of theoretical cone angle-frequency relationship (2.19) for the indicated values of the parameter ω_p/ω_c. The solid circles represent experimental data taken at a magnetic field corresponding to a cyclotron frequency $f_c = 800$ MHz. The cone angle is observed to steadily increase with frequency in the lower branch $\omega < \omega_c$, and then decrease in the upper branch $\omega_p < \omega < \omega_{uh} = (\omega_c^2 + \omega_p^2)^{1/2}$. From this data we conclude that $\omega_p/\omega_c \simeq 1$, or $f_p = 800$ MHz, or that the electron density is $n_e \simeq 8 \cdot 10^9 e/cm^3$.

Figure 4.4 shows cone angle data taken at a lower magnetic field ($f_c = 480$ MHz). Now $\omega_p > \omega_c$, and the lower branch ($\omega < \omega_c$) and upper branch ($\omega_p < \omega < \omega_{uh}$) are clearly separated by a frequency region ($\omega_c < \omega < \omega_p$) in which, as predicted, no cones are present. From this data we see that $\omega_p/\omega_c \simeq 1.5$ or $f_p \simeq 720$ MHz corresponding to $n_e \simeq 6.5\ 10^9 e/cm^3$. For $\omega_p < \omega_c$ cones were also observed to exist in a lower branch ($\omega < \omega_p$) and an upper branch ($\omega_c < \omega < \omega_{uh}$), as expected.

An independent measurement of the plasma density was made using a 10.5 GHz microwave interferometer. Two external waveguide horns were used to study the propagation of an ordinary wave ($\vec{E} \,||\, \vec{B}_o$) across the plasma column. The phase shift introduced by the presence of the plasma is

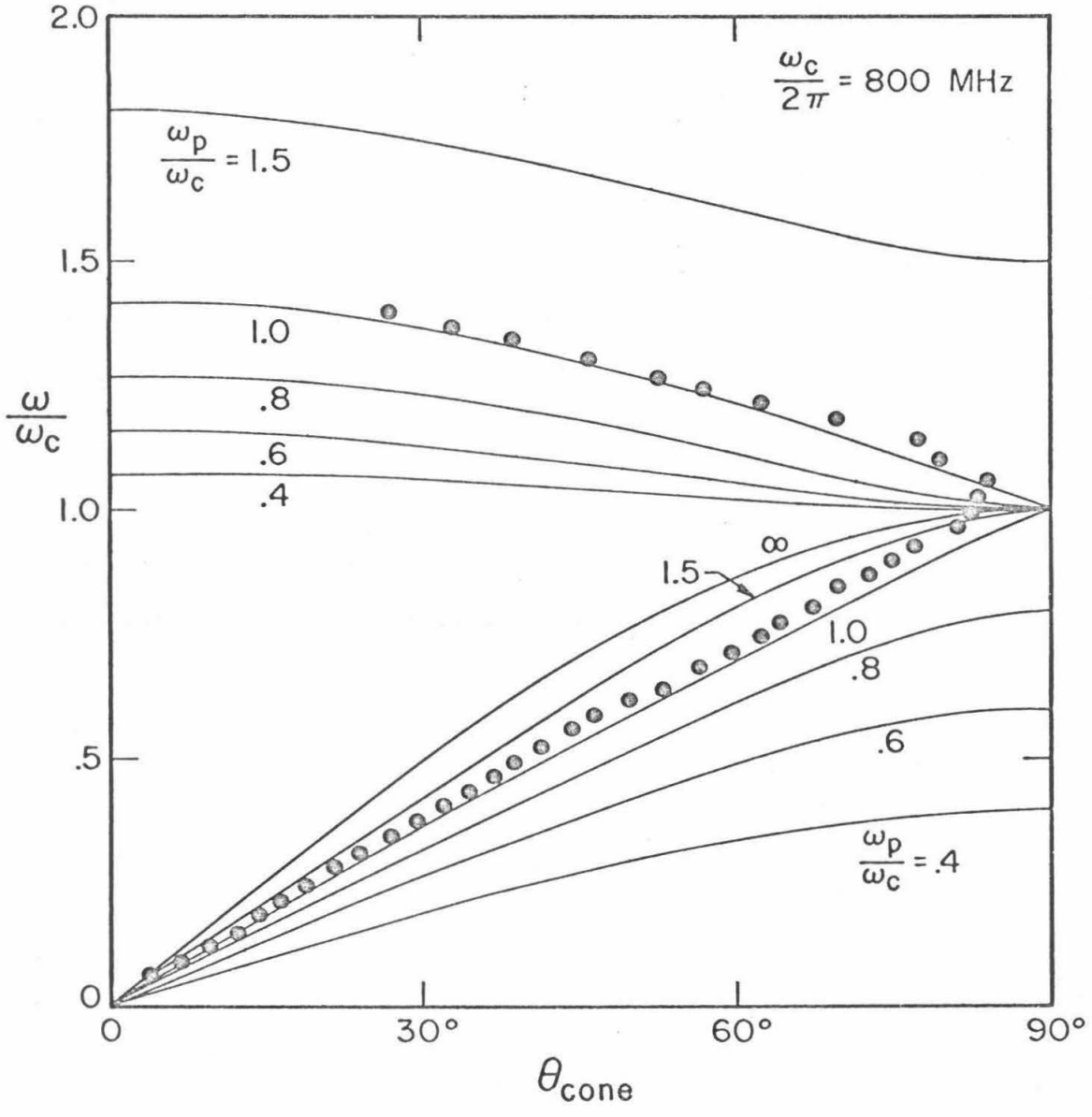

Fig. 4.3 Experimentally observed location of resonance cone angle versus the ratio ω/ω_c for $\omega_p \simeq \omega_c$. Solid curves are those predicted by Eq. 2.19 for labeled values of ω_p/ω_c.

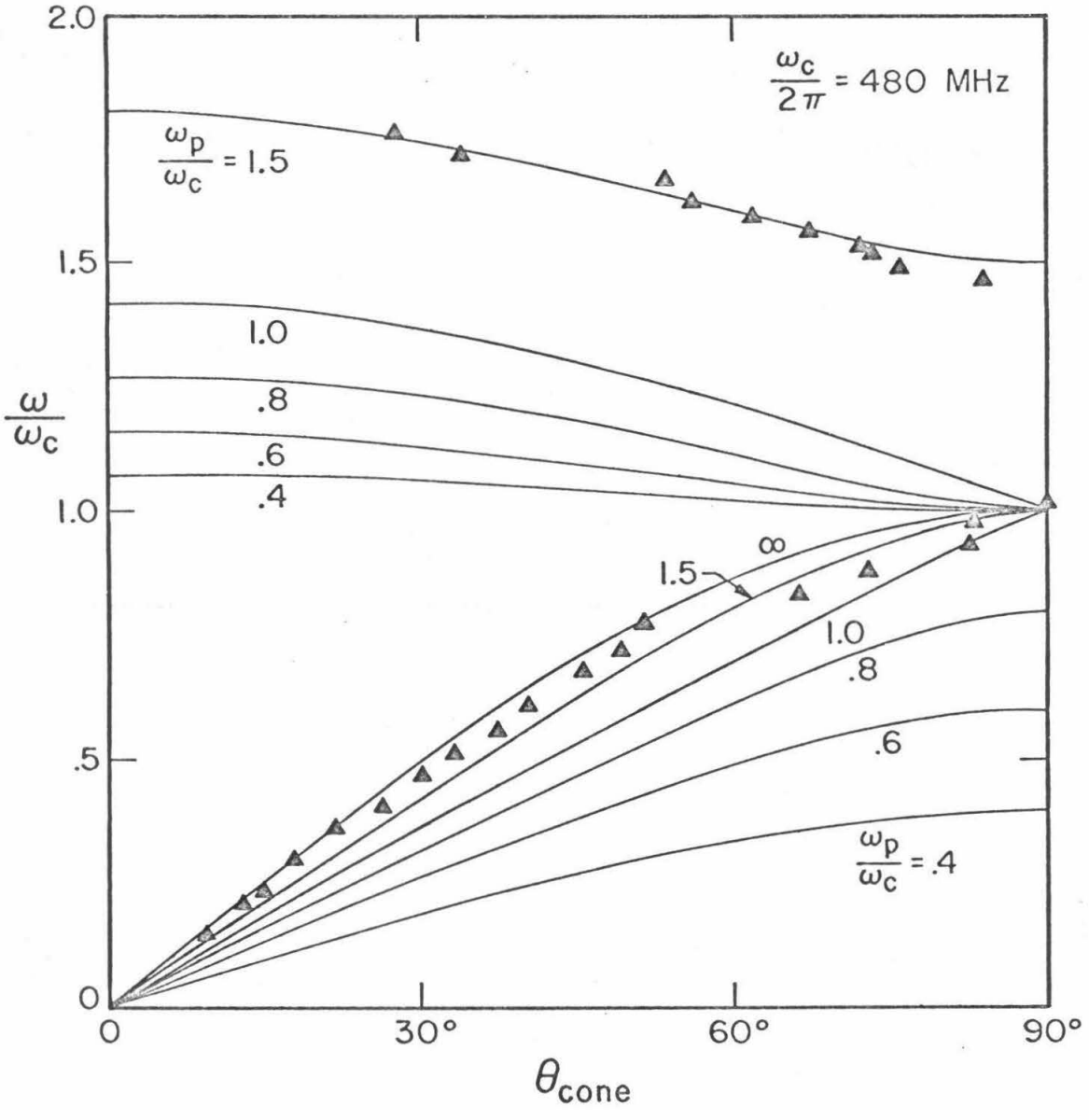

Fig. 4.4 Experimentally observed location of resonance cone angle versus the ratio ω/ω_c for $\omega_p \simeq 1.5\,\omega_c$. Lower and upper branches clearly separated by frequency region in which, as predicted, no cones are present.

$$\Delta\Phi \simeq \frac{\pi L}{\lambda \omega^2} \langle \omega_p^2 \rangle \tag{4.1}$$

where ω is the incident frequency, λ is the free-space wavelength, L is the length of the transmission path through the plasma and $\langle \omega_p^2 \rangle$ is a measure of the average plasma density across the column [30]. Figure 4.5 compares f_{p_c} calculated from the experimentally measured cone angle to $(\Delta\Phi)^{1/2}$ for two different magnetic fields. As we increased the rf power producing the plasma (points 1 → 3), the two measurements were seen to remain in a constant proportion for a given magnetic field. Also the plasma frequency calculated from the interferometer measurement f_{p_Φ} agreed with the plasma frequency calculated from the cone angle measurement f_{p_c} to within 11% . The different slopes in Fig. 4.5 are believed due to a change in density profile with static magnetic field strength. The phase shift $\Delta\Phi$ measures $\langle \omega_p^2 \rangle$ across the entire plasma diameter, while θ_c measures $\langle \omega_p^2 \rangle$ only between the transmitting and receiving probe. The average plasma density between the probes relative to the average density across the entire diameter probably increases as the magnetic field decreases.

The agreement between experiment and theory shown in Figs. 4.3 and 4.4 appears to indicate that the plasma density radial profile was relatively uniform in the experimental plasma column, at least out to a radius equal to the probe separation in those measurements (approximately 6 cm). As a check the cone angles were measured using four different receiving probes, each at different radii (approximately 1, 2, 3 and 6 cm), and most of the measurements agreed to within 2-3°, indicating that the plasma density was uniform to within 10-20% in this region.

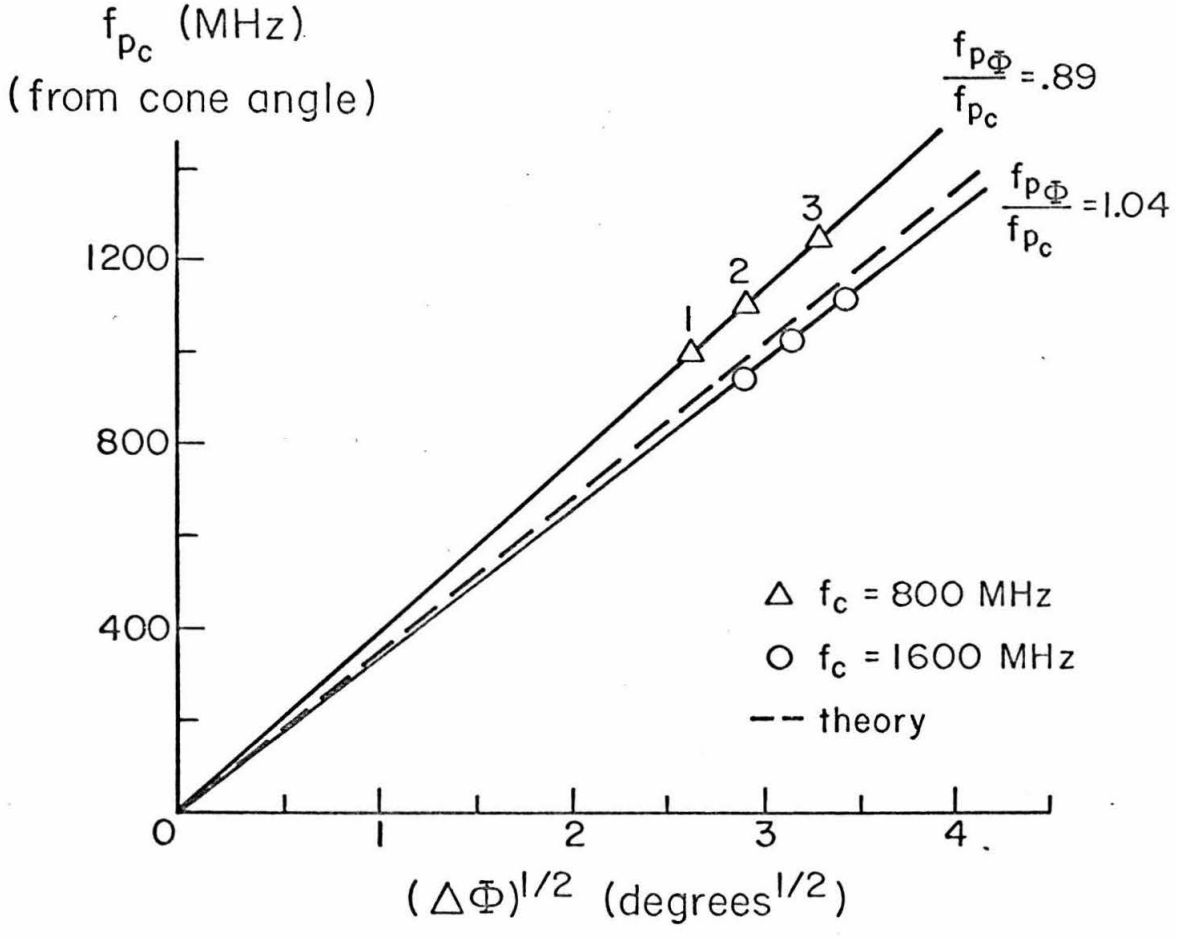

Fig. 4.5 Comparison of the plasma frequency f_{p_c} calculated from the cone angle measurements to f_{p_Φ} measured using a microwave interferometer. $\Delta\Phi$ is the phase shift measured by the interferometer.

The above results show that the resonance cone angle can be used as a diagnostic measure of the plasma density in a plasma in a magnetic field. The upper branch especially is very dependent on the electron density. Since the theory of Langmuir probes is not completely understood in the presence of a magnetic field, and since many plasmas are too small to be reliably analyzed using a microwave interferometer, the resonance cone measurement could be a very useful diagnostic tool. Very little equipment is required: an oscillator chosen in the proper frequency range, transmitting and receiving probes (which could both be entered through the same port), and a detection system (which could be as simple as a crystal detector and DC voltmeter if the probe separation were small enough). The minimum distance between the probes is limited by the debye length in the plasma and the loss in angular resolution as the probe separation decreases. Cone angle measurements have been easily made with probe separations as small as 1.3 cm.

4.2 Amplitude and Phase Measurements

The relative amplitude (on a logarithmic scale) and phase of the received signal were measured using the HP8410A network analyzer as shown in Fig. 3.3. Examples of characteristic X-Y recorder traces are shown in Figs. 4.6 and 4.7. The resonance cone amplitude was usually 10-20 db above the lowest level signal. The signal level inside the resonance cones was observed to be larger than that outside the cones for lower branch cone angles less than about 40-50^{o}, but as

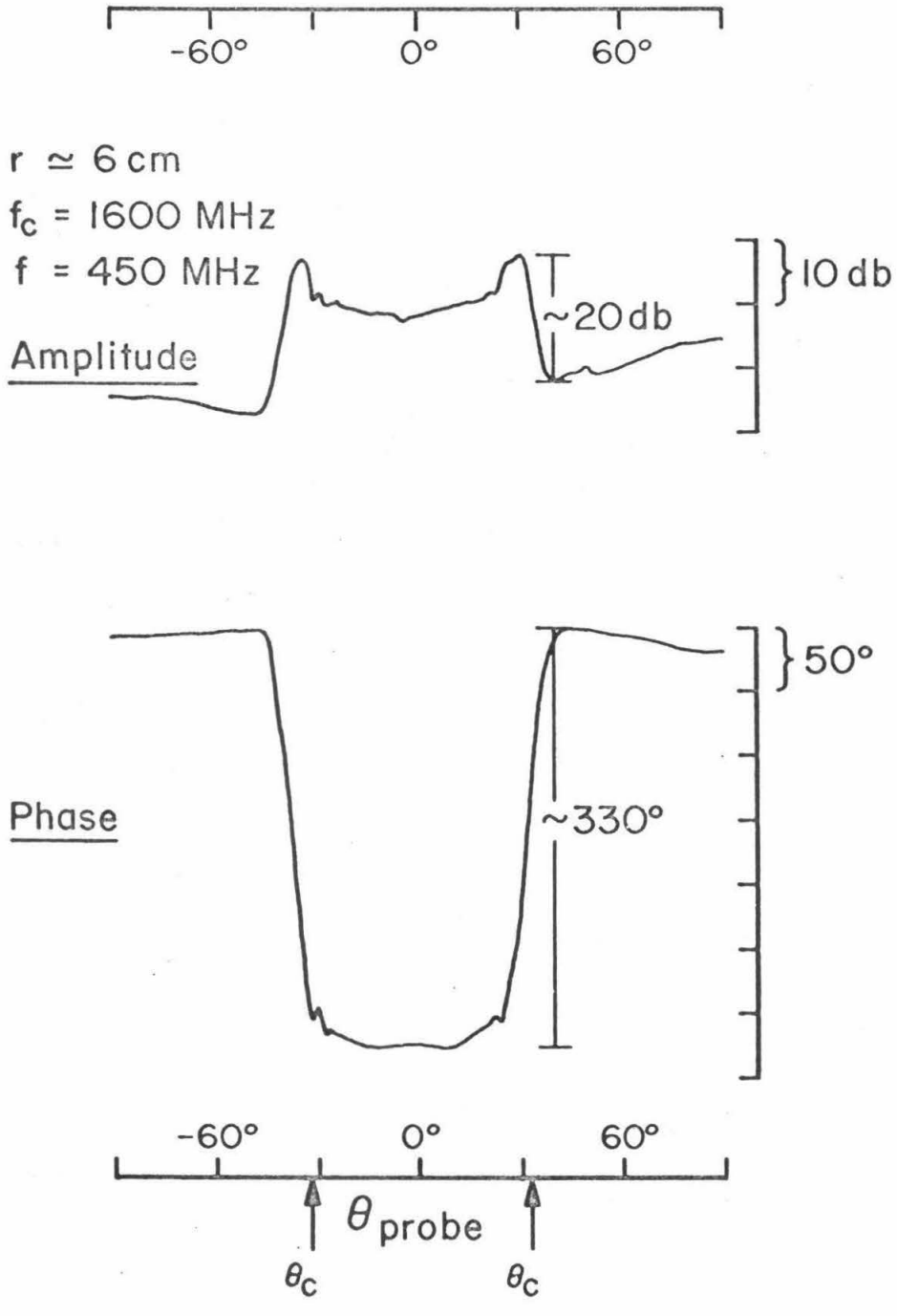

Fig. 4.6 Experimental traces showing relative amplitude on a logarithmic scale and phase of received signal versus θ_{probe} for r = 6 cm, f_c = 1600 MHz and f = 450 MHz. The signal undergoes a large phase shift as θ_p passes through the resonance cone angle θ_c .

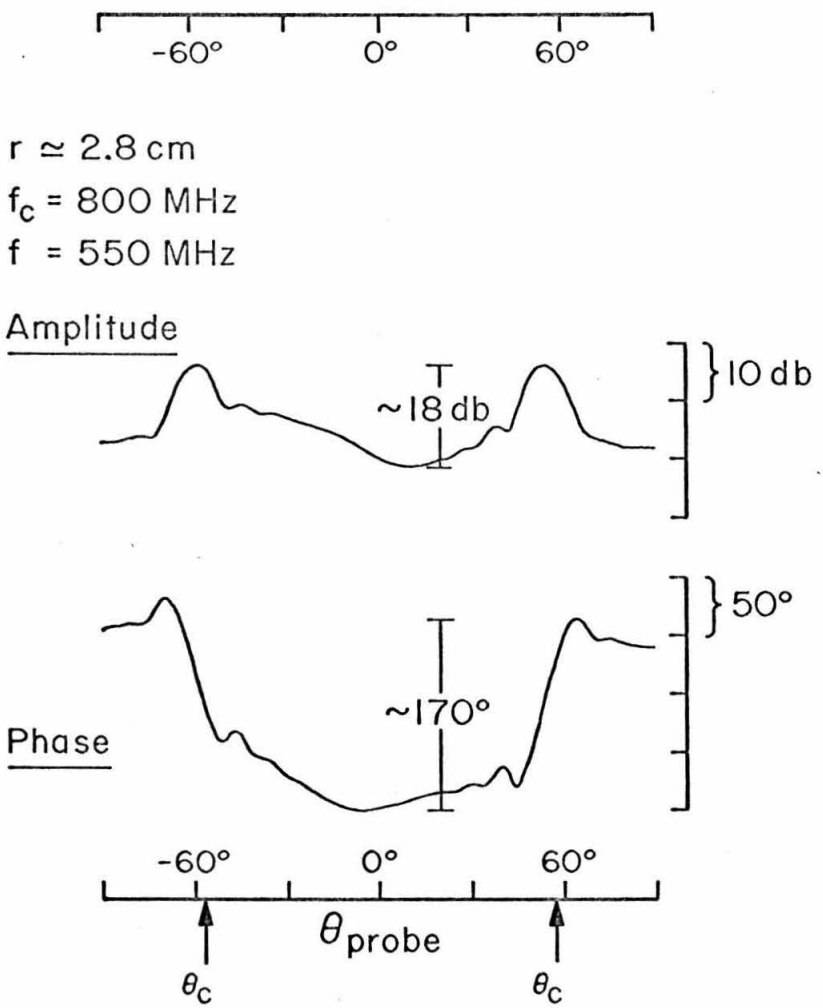

Fig. 4.7 Experimental traces showing relative amplitude on a logarithmic scale and phase of received signal versus θ_{probe} for r = 2.8 cm, f_c = 800 MHz and f = 550 MHz.

the cone angle was increased further, this difference in levels slowly vanished.

The phase of the received signal changed markedly as the receiving probe passed through the resonance cone. The magnitude of this phase shift varied between about 150^{o} and 400^{o}. These phase measurements gave the first indication that the probes used in these experiments did not behave as simple dipoles.

If the probes were simple dipoles, the receiving probe would measure the electric field of the transmitting probe. The near-zone electric field of an oscillating dipole can be obtained by taking two spatial derivatives of equation (2.16), one in the direction of the dipole to obtain the dipole potential and one in the direction of the desired component of the electric field. This would result in an electric field proportional to r^2/R^5 where $r = (\rho^2 + z^2)^{1/2}$ and $R = [K_{||}\rho^2 + K_{\perp}z^2]^{1/2}$. Since R^2 changes sign in passing through the resonance cone, the phase of the electric field should change by $5/2(180^{o}) = 450^{o}$. Effects such as electron collisions and electron thermal velocities added to the theory would make the phase change gradual and slightly less than 450^{o}. In the far zone, Kuehl [5] shows that the electric field is proportional to r^2/R^3 so that a phase shift of $3/2(180^{o}) = 270^{o}$ would be expected. Considering a uniaxial plasma for simplicity, Clemmow [10] finds that the field at an arbitrary distance has terms proportional to r^2/R^3, r^2/R^4 and r^2/R^5. This would allow a phase shift anywhere between 270^{o} and 450^{o} at intermediate distances. Here the terms near-zone and far-zone refer

to the size of $\omega r/c$ which in these experiments was usually less than or about equal to unity. The quantity which enters in the expressions for the fields, however, is $\omega R/c$ whose magnitude varied from zero on the resonance cone to infinity near $\omega = 0$ and $\omega = \omega_c$.

The measured phase shift in passing through the resonance cone was about 300°-400° under most conditions for a probe separation of approximately 6 cm (see Fig. 4.6). For cone angles less than about 20-30°, there was a transition from this type of characteristic phase trace to traces where the phase would first increase and then decrease in passing through the cone, so that the total phase shift between the signal inside the cone and outside the cone was very small. For a probe separation of approximately 2.8 cm, the measured phase shift was only about 150°-200°. These experimental results are not consistent with the theory presented above. In Section VI the addition of electron thermal velocities to the theory shows that there are really two waves contributing to the received signal, a fast electromagnetic wave and a slow plasma wave. The phase of each of these waves changes independently with angle and the interference between the waves causes the total signal to become very small at times. The total phase shift in passing through the resonance cone will depend on the relative amplitude of the slow and fast waves which depends on the damping in the plasma and sheath effects around the exciting probe, making comparisons between experiment and theory very difficult. N. Singh [31] has calculated the fields of an oscillating dipole in a warm uniaxial plasma and has obtained angular phase patterns which are similar to

the experimental traces.

The experimental probes did not behave as simple dipoles. This was confirmed when the probes did not produce a 180^{o} phase change in the transmitted signal when the assumed dipoles were tested in air by first holding them parallel and then antiparallel. In order to make quantitative comparisons of the field pattern with theory (especially in Section VI), it would have been desirable to construct true dipole antennas. Several attempts were made and some of these are discussed in Appendix C. Most antennas designed to behave as dipoles at distances large compared to the size of the antenna, must have dimensions on the order of a half-wavelength, and this was not practical in this experiment since the free space wavelengths are $\simeq$ 20 cm.

In Section II it was shown that the cones should be present regardless of the charge distribution on the exciting probe. In the attempts to construct true dipole probes, a variety of probe designs and orientations were investigated and the qualitative features of the resonance cones were always observed, as expected.

V. PHASE AND GROUP VELOCITY IN AN ANISOTROPIC PLASMA

The theory of plane wave propagation in an anisotropic plasma has been widely discussed [32]. The index of refraction and wave vector $\underline{k}$ become singular at a certain angle ψ_c which the wave vector makes with respect to the static magnetic field direction, and this angle is sometimes also referred to as the resonance cone angle.* This resonance angle ψ_c is the complementary angle of the physical angle θ_c, at which the fields of a small source in a magnetoplasma become singular. This difference is not widely appreciated and is explained below in terms of the directions of the phase and group velocities of waves in an anisotropic plasma.

In the study of plane wave propagation in an anisotropic plasma, the results are usually presented in the form of a Clemmow-Mullaly-Allis (CMA) diagram (see Fig. 5.1).** This is a two-dimensional parameter space with the vertical axis ω_c^2/ω^2 and the horizontal axis ω_p^2/ω^2. The solid lines (resonances, phase velocity $v_p \to 0$) and the dashed lines (cutoffs, $v_p \to \infty$) divide the parameter space into different regions. In each region the principal waves which are present are indicated by the symbols ℓ, r, o and x which

---

*The possibility of confusion is indicated in that Tunaley and Grard [21] erroneously state that the fields of a source in an anisotropic plasma should exhibit resonance cones at angle ψ_c.

**For a more detailed explanation of the CMA diagram than will be given here, see Allis, Buchsbaum, and Bers, Reference [32].

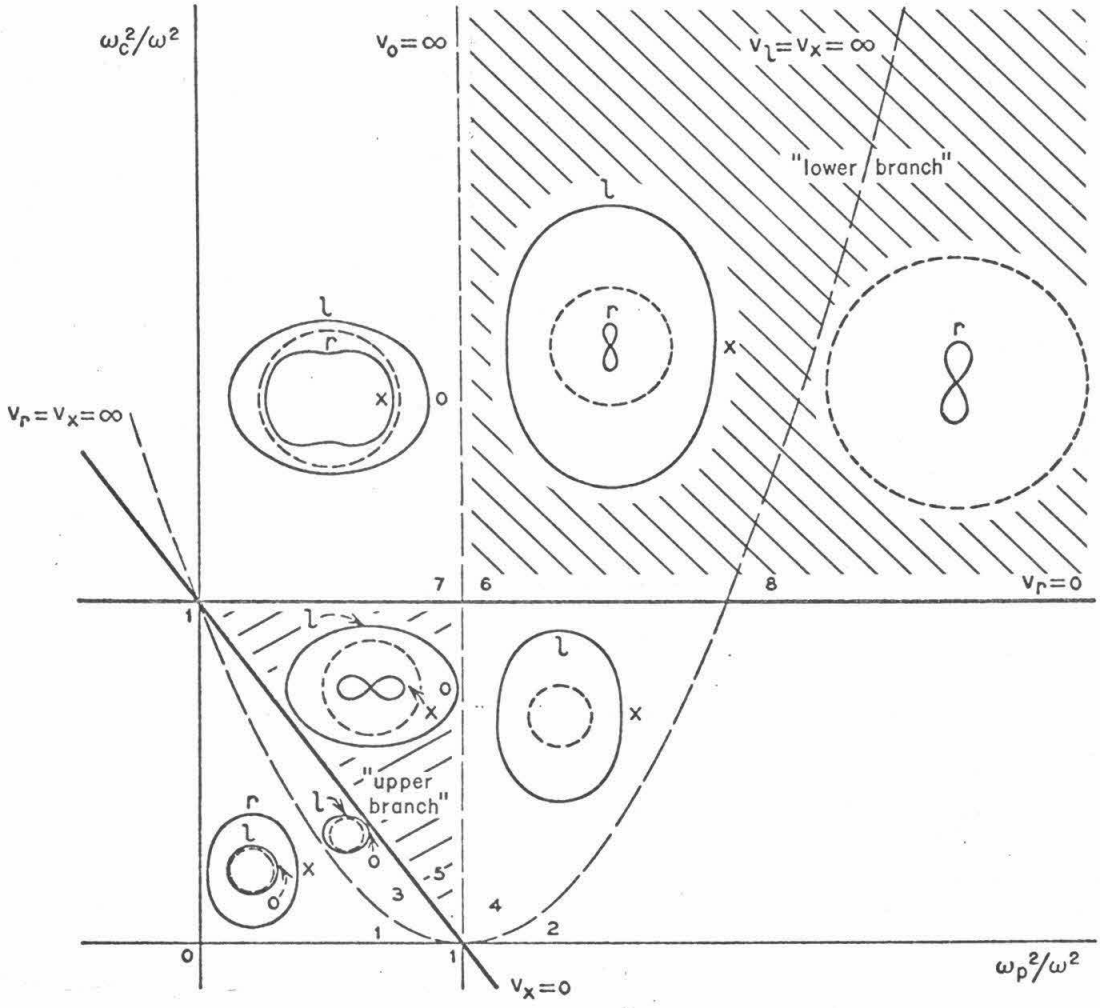

Fig. 5.1 CMA diagram for an electron plasma ($m_{ion} \to \infty$). This two-dimensional parameter space is divided into different regions, and characteristic wave-normal surfaces are sketched for each region. The regions of interest are shaded.

refer to the polarization of these waves in the limit of propagation along the field (ℓ = left circularly polarized and r = right circularly polarized) and across the field (o = ordinary, polarized along B_o and x = extraordinary, polarized across B_o). Since one of the principal waves appears or disappears whenever a cutoff or resonance line is crossed, the phase velocity surface is topologically different in each of eight regions of the parameter space. It is significant, therefore, to sketch a typical phase velocity surface for each region. These sketches show the magnitude of the phase velocity v_p versus the angle ψ which the phase velocity makes with respect to the static magnetic field direction (which is vertical in these diagrams). As the regions are very different in size, it is necessary to sketch each plot on a different scale, and this is shown in each case by the dotted circle that represents the velocity of light.

In the frequency region corresponding to the lower branch of the cones ($\omega < \omega_p, \omega_c$), regions 6 and 8 in Fig. 5.1, propagation is allowed only for $\psi < \psi_c$. Outside the limiting cone $\psi = \psi_c$ the waves are evanescent, i.e., there are no propagating waves. $\psi = \psi_c$ is called a resonance cone because the index of refraction $n \to \infty$ ($v_p \to 0$) on the cone. We refer to this as the phase velocity cone [33]. In the frequency region corresponding to the upper branch of the cones ($\omega_p, \omega_c < \omega < \omega_{uh}$), propagation is allowed only for $\psi > \psi_c$. This interchange is due to the change in sign of both $K_\perp$ and $K_\parallel$ for the plasma. On the other hand, Kuehl [5] in discussing the fields of an oscillating point dipole in a uniaxial plasma ($B_o \to \infty$, for which there is no upper branch) shows that for the lower branch ($\omega < \omega_p$) the

Poynting vector is non-zero only for $\theta < \theta_c$. So there is an apparent paradox in deciding the possible directions of propagation with respect to the magnetic field in a plasma. For example, consider a probe exciting waves of frequency $\omega = \sqrt{3}\,\omega_p/2$ in a plasma with $\omega_c >> \omega_p$. The wave vector $\underline{k}$ of the waves, sometimes called the propagation vector, is real only at angles $\psi < \psi_c = 30^o$ which the wave vector makes with respect to the magnetic field direction, and the waves are evanescent for $\psi > 30^o$. However, the Poynting vector is non-zero out to angles $\theta < \theta_c = 60^o$, and in fact the field is largest at $\theta = 60^o$, so there definitely is propagation at angles greater than 30^o.

The resolution of this paradox is found if we remember that in an anisotropic plasma the directions of the phase velocity $\underline{v}_p = \frac{\omega}{k}(\underline{k}/k)$ and group velocity $\underline{v}_g = \partial\omega/\partial\underline{k}$ are generally different. Considering a <u>uniaxial</u> plasma ($B_o \to \infty$) for simplicity, the dielectric constants become

$$K_\perp = 1 \quad \text{and} \quad K_{||} = 1 - \omega_p^2/\omega^2 \tag{5.1}$$

so that:

$$\sin^2\theta_c = \omega^2/\omega_p^2 \tag{5.2}$$

For this case it can be shown that as the angle ψ of the phase velocity increases from 0 to ψ_c, the angle θ of the group velocity increases from 0 to $\theta_c = \pi/2 - \psi_c$ (see Appendix E). This behavior is illustrated in Fig. 5.2. The <u>right</u> half is a polar plot of $\underline{v}_p/c$ for $\omega_p/\omega = 2$ or $\psi_c = 60^o$. (The dots correspond to 5^o increments in ψ). The <u>left</u> half of Fig. 5.2 is a polar plot of $\underline{v}_g/c$ for the

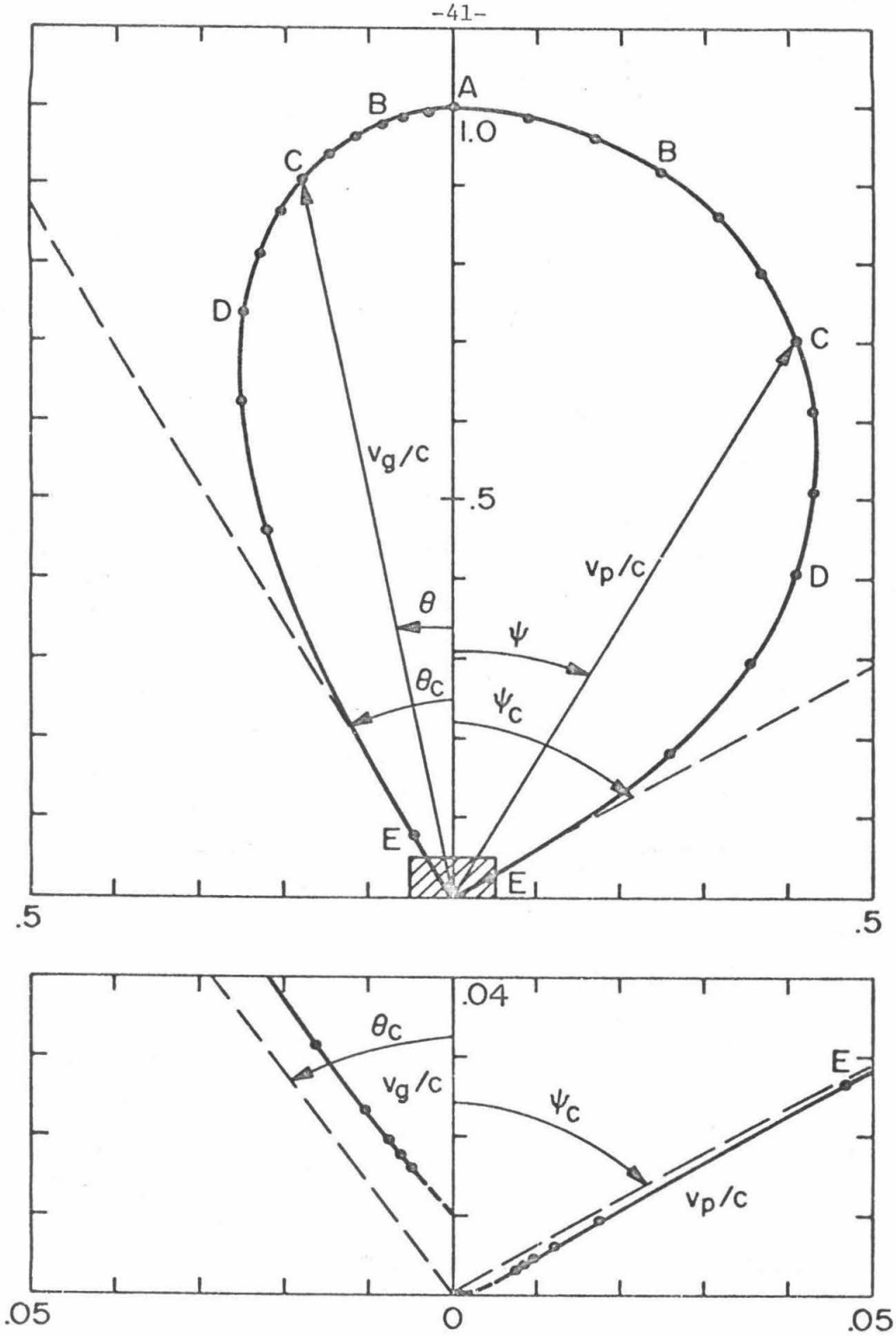

Fig. 5.2 Polar plot of phase velocity (right side) and group velocity (left side) for $B_o = \infty$, $\omega_p/\omega = 2$. Lower plot shows shaded region, where electron thermal velocities are important, on an expanded scale.

same conditions. Each dot on the group velocity plot is to be associated with the corresponding dot on the phase velocity plot (e.g., A,B,C,$\cdots$). Thus θ_c defines a second cone within which the group velocity must lie and on which it tends to zero. We refer to this cone as the group velocity cone [33]. It can also be shown that the phase and group velocities are perpendicular on the resonance cone for a finite magnetic field (see Appendix B).

Although the group velocity vanishes as $\theta \to \theta_c$, the energy density and Poynting vector become singular, leading to the experimentally observed cones. Since propagation between two remote points in a plasma is determined by the group velocity, the importance of the group velocity and hence the group velocity cone rather than the customary phase velocity plots and cone should be emphasized. While this experiment was not performed in the far field region, the observed cone angles are those predicted by considerations of the group velocity and fields in the far zone.

VI. WARM PLASMA EFFECTS

6.1 Addition of Electron Thermal Velocities to the Theory

We will again consider the quasi-static potential of an oscillating charge for simplicity. The solution obtained will be valid near the resonance cones. For a warm plasma ($2KT_e = mv_{th}^2$), the plasma dielectric constants $K_\perp$ and $K_{||}$ become functions of the wave vector $\underline{k}$ and the inverse Fourier integral for the potential (Eq. 2.8) could most easily be evaluated in the limit of a large static magnetic field ($B_o \to \infty$). Experimentally this condition corresponds to $\omega_c >> \omega_p, \omega$. In this limit

$$K_\perp = 1 \qquad \text{and} \qquad K_{||} = 1 - \frac{\omega_p^2}{k_{||}^2 v_{th}^2} Z'\left(\frac{\omega}{k_{||} v_{th}}\right) \tag{6.1}$$

where Z' is the derivative of the plasma dispersion function with respect to its argument [34]. The integrations over ϕ and $k_\perp$ are performed as before and equation (2.12) becomes

$$\phi(\rho,z) = \frac{qe^{-i\omega t}}{4\pi^2 \varepsilon_o} \int_{-\infty}^{\infty} K_o(k_{||} \rho \sqrt{K_{||}}) \, e^{ik_{||} z} \, dk_{||} \tag{6.2}$$

Numerical evaluation of this integral using an IBM 360 computer yields the cone structure shown in Fig. 6.1. (Note--a subroutine for calculating Z' is required.) Three important effects are observed. First, the potential now remains finite at the resonance cone. Second, the cone angle θ_c is shifted to a slightly smaller angle than that predicted by cold plasma theory ($\theta_c = \sin^{-1} \omega/\omega_p$). This is the probable explanation for the consistent trend evident in Figs. 4.3 and

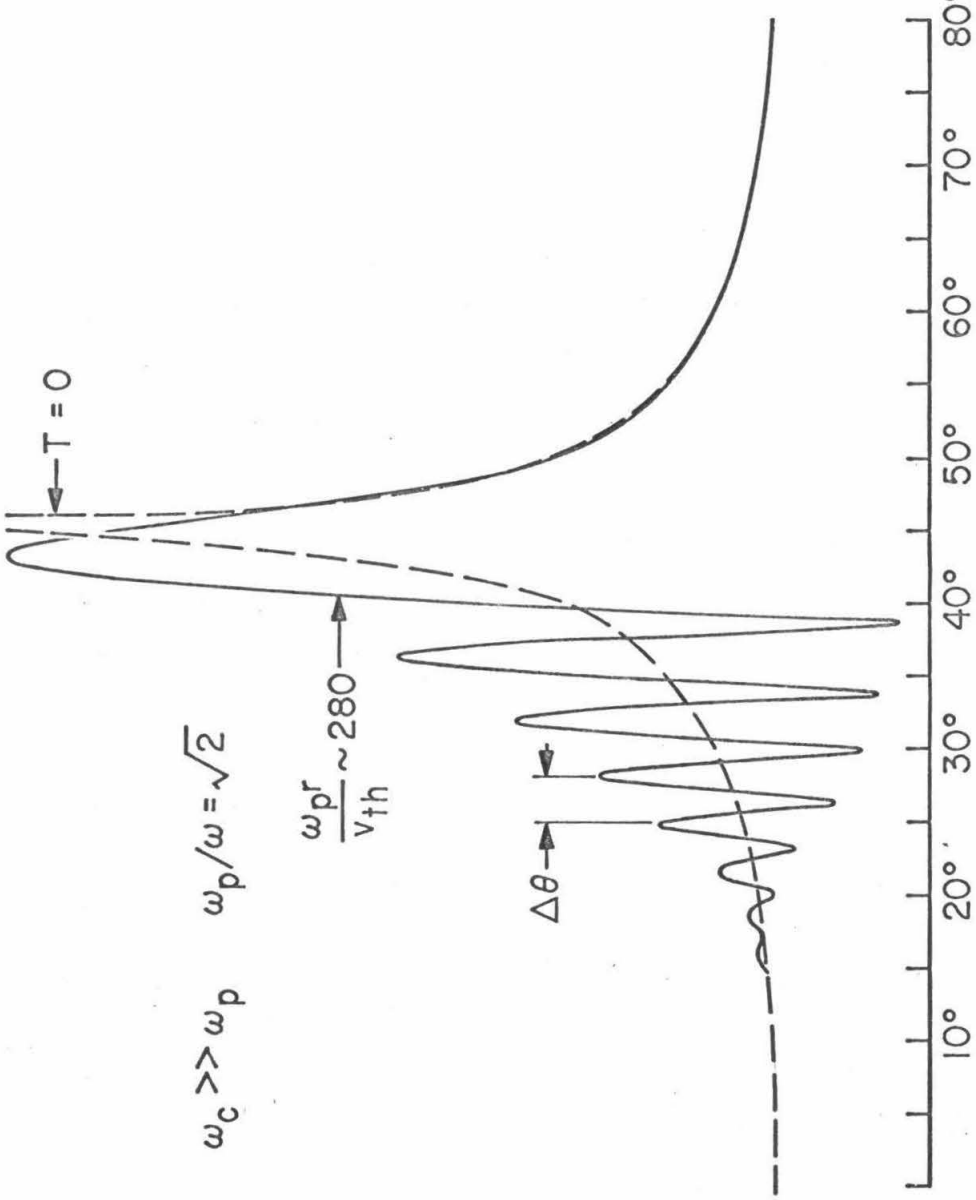

Fig. 6.1 Calculated angular dependence of the potential $|\phi(\theta)|$ for $v_{th}/\omega_p r = 1/280$ (solid curve) and for $v_{th}/\omega_p r = 0$ (dashed curve).

4.4 where the experimental points seem to fall at a slightly smaller angle than that which would give the best agreement with theory, with the upper and lower branches both falling nearer to a given ω_p/ω_c theoretical line. Third, and most interesting, an interference structure appears inside the cones. An empirical fit to the numerical data or evaluation of equation (6.2) by the method of stationary phase (see Appendix D) shows that the angular spacing between any two adjacent maxima in the interference structure is $\Delta\theta \propto (v_{th}/\omega_p r)^{2/3} \tan^{1/3}\theta_c$ where r is the distance between the probes. The angular spacing is largest between the resonance cone and the first maximum of the interference spacing and then becomes smaller for the spacing between the first and second maxima and remains relatively constant, the spacing between adjacent maxima further from the cone decreasing only slightly.

N. Singh [31] has done a calculation of the fields of an oscillating dipole in a warm uniaxial plasma based on the full set of Maxwell's equations and obtains a similar relationship for the interference spacing.

This structure is due to an interference between a fast electromagnetic wave ($v_g \sim c$) and a slow plasma wave ($v_g \sim v_{th}$). The left lower portion of Fig. 5.2 shows that the addition of electron thermal velocities modifies the group velocity polar plot so that inside the resonance cone ($\theta < \theta_c$) for each direction θ there are two solutions, a fast wave and a slow wave. The right portion shows that the phase velocity is now non-zero at all angles ψ. The phase of the slow wave changes very rapidly with θ, yielding the interference pattern. This is because near the cones the phase velocity is nearly

perpendicular to the group velocity, i.e., the phase velocity is in the θ-direction. In the electrostatic solution the slow wave is interfering with a fast "wave" which arrives instantaneously ($c \to \infty$).

6.2 Experimental Results

The interference structure inside the cones was indeed observed experimentally and is present in Figs. 4.1 and 4.2. It was not as pronounced as shown in the theoretical curve in Fig. 6.1, but the amplitude of the interference structure depends on the relative amplitude of the slow and fast waves, which in turn depends on the type of probe exciting the waves, the damping mechanisms in the plasma [31] and the sheaths around the probes [35], making quantitative amplitude comparisons of theory and experiment impractical. The angular interference spacing is, however, dependent only on the relative phase of the slow and fast waves [31] and does not depend significantly on the type of probe used.

The interference structure was also observed in the phase of the received signal near the cone angle (see Figs. 4.6 and 4.7). Under most experimental conditions the phase interference amplitude was relatively small, indicating that the plasma wave contribution to the total signal was small compared to the electromagnetic wave contribution. The measured angular interference spacing in the phase pattern was identical to that in the amplitude pattern, as expected. The interference was most prominent in both the phase and amplitude measurements at intermediate cone angles (θ_c between approximately 30^o and 60^o).

Having shown that the angular interference spacing could most easily be used to test the theory, detailed measurements of this spacing were undertaken. The static magnetic field was kept as large as possible ($\omega_c \gtrsim 2.3\omega$) to best approximate the limit $B_o = \infty$. An empirical fit to the numerical calculations of the integral given in equation (6.2) for the potential of an oscillating charge shows that the spacing between the first few successive maxima* of the interference structure is given by

$$\Delta\theta = 5.8^o \left(\frac{200}{\omega_p r/v_{th}}\right)^{2/3} \tan^{1/3} \theta_c \qquad (6.3)$$

Knowing the probe separation r and the resonance cone angle θ_c (and hence the plasma frequency ω_p from equation (2.19)), the experimentally measured angular spacing $\Delta\theta$ and equation (6.3) can be used to find the electron thermal velocity v_{th} and hence the electron temperature T_e. From a large number of measurements of the angular spacing taken at various probe separations and at various cone angles, use of equation (6.4) indicated an electron temperature T_e between 2 and 4eV with most measurements between 2 and 3 eV.

An independent measurement of the electron temperature was made using both cylindrical and disc single Langmuir probes. The results were interpreted assuming the electron velocity distribution in the

---

*Note that this does not apply to the spacing between the first maximum and the resonance cone itself. The constant of proportionality is then 8.7^o rather than 5.8^o.

plasma was both Maxwellian and isotropic. The electron temperature was obtained from the slope of a semilogarithmic plot of the current collected by the probe versus the applied voltage. Simple Langmuir probe theory fails when a strong magnetic field is present, but by using only the very small current portion of the current-voltage probe characteristic, only those electrons within a few cyclotron radii are sampled and their collection is not substantially affected by the imposed static magnetic field. This has the disadvantage, however, of only sampling the high energy tail of the electron distribution and it is not certain that the energy distribution in the plasma was Maxwellian. In addition, the imposed static magnetic field may cause velocity distribution to be anisotropic, and this leads to a further uncertainty in the probe measurements. And finally, it must be remembered that the Langmuir probe is measuring a different property of the electron energy distribution function than is the angular interference spacing measurement. The Langmuir probe results depend only on the high-energy tail of the distribution function, while the angular spacing depends only on the mean-square value of the electron thermal velocity, since for $k^2\overline{v^2} \ll \omega^2$, the correction to the plasma dielectric constant to first order in the temperature involves only $\overline{v^2}$. The Langmuir probe measurements yielded an electron temperature of about 3-5eV. The disc probe yielded the most well defined ion saturation current and probably the best measure of the electron temperature, about 3eV, and this is in fairly good agreement with that calculated from the angular interference spacing.

To further test the theory, four receiving probes were constructed, each at a different radius from the transmitting probe in order to verify that $\Delta\theta \propto r^{-2/3}$. Typical experimental results showing the decreasing interference spacing with increasing probe separation are presented in Fig. 6.2. In Fig. 6.3 the triangular points are the measured angular spacing between the first maximum of the interference spacing and the cone; the circular points that between the second maximum and the cone. Both sets of experimental points are consistent with the $r^{-2/3}$ dependence. Similar data, taken under a variety of plasma conditions, when plotted on a log-log plot and fitted to a straight line by a least squares procedure, yielded an average slope $-.74 \pm .05$. This somewhat higher value than the expected -2/3 may be due to perturbations on the plasma due to the presence of the probes. If the slow plasma wave is assumed to be launched and detected at the edge of the probe sheaths, this would decrease the effective distance between the probes. Using a sheath thickness of five Debye lengths and replotting the data yields a corrected average slope $-.70 \pm .04$. Another effect, and one which cannot easily be quantitatively taken into account, is that the average plasma density between two probes should decrease as the probe separation decreases. This would also cause the experimental slope to be too large.

Measurements of the interference spacing as a function of cone angle were also taken and the results are presented in Fig. 6.4. The vertical axis is $r^{2/3}\Delta\theta$ so that data taken at three different probe separations could be presented on a single plot; the triangular points were taken with $r \simeq 1.3$ cm, the circular points with $r \simeq 2.8$ cm, and

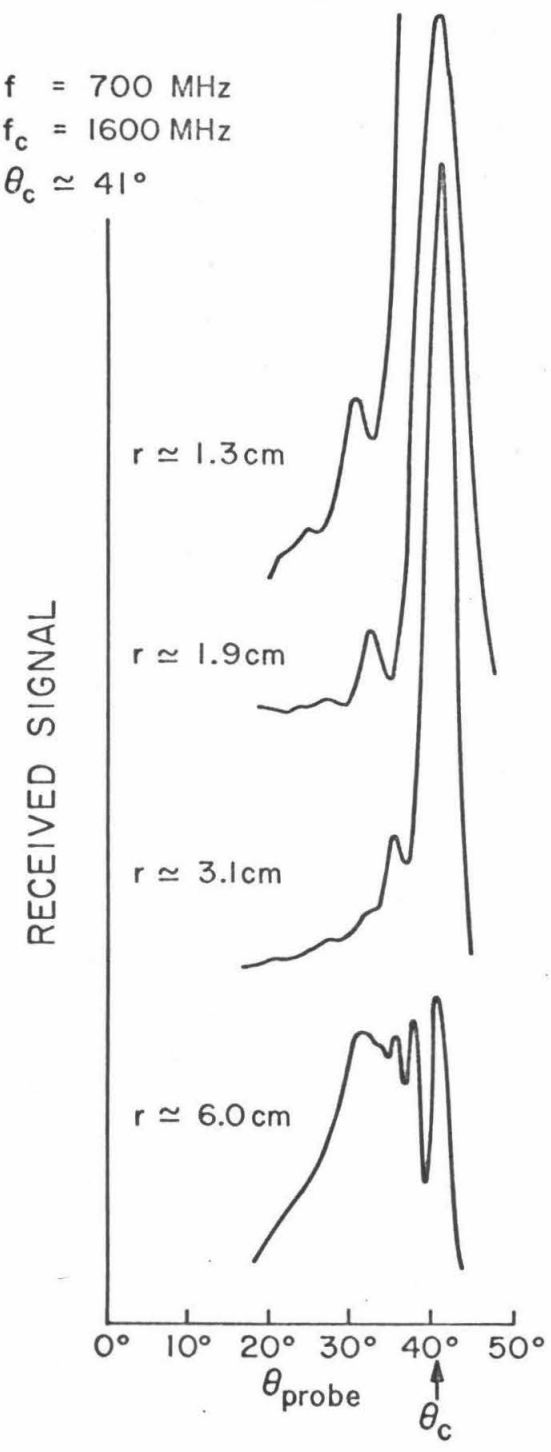

Fig. 6.2 Portions of experimental traces showing decreasing interference spacing $\Delta\theta$ with increasing probe separation.

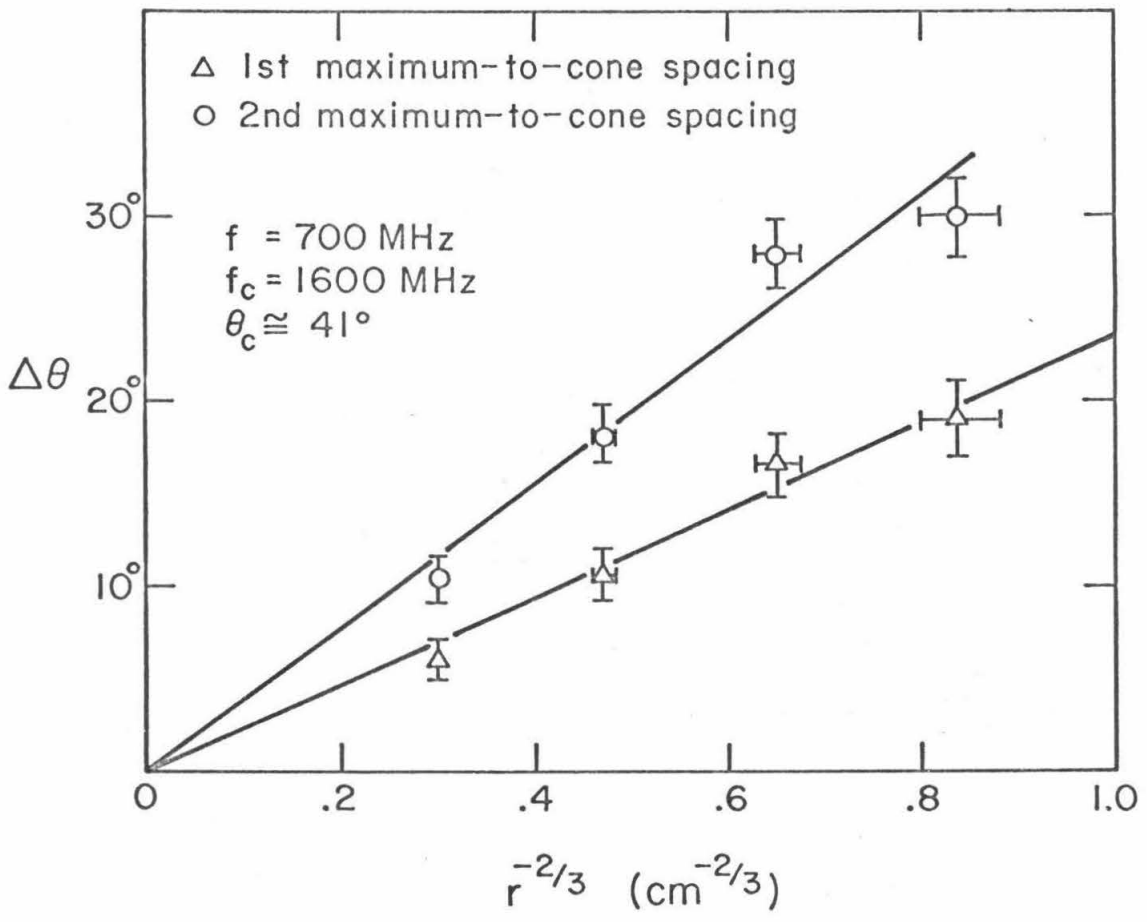

Fig. 6.3 Experimental interference spacing $\Delta\theta$ versus $r^{-2/3}$, where r is the distance between the probes.

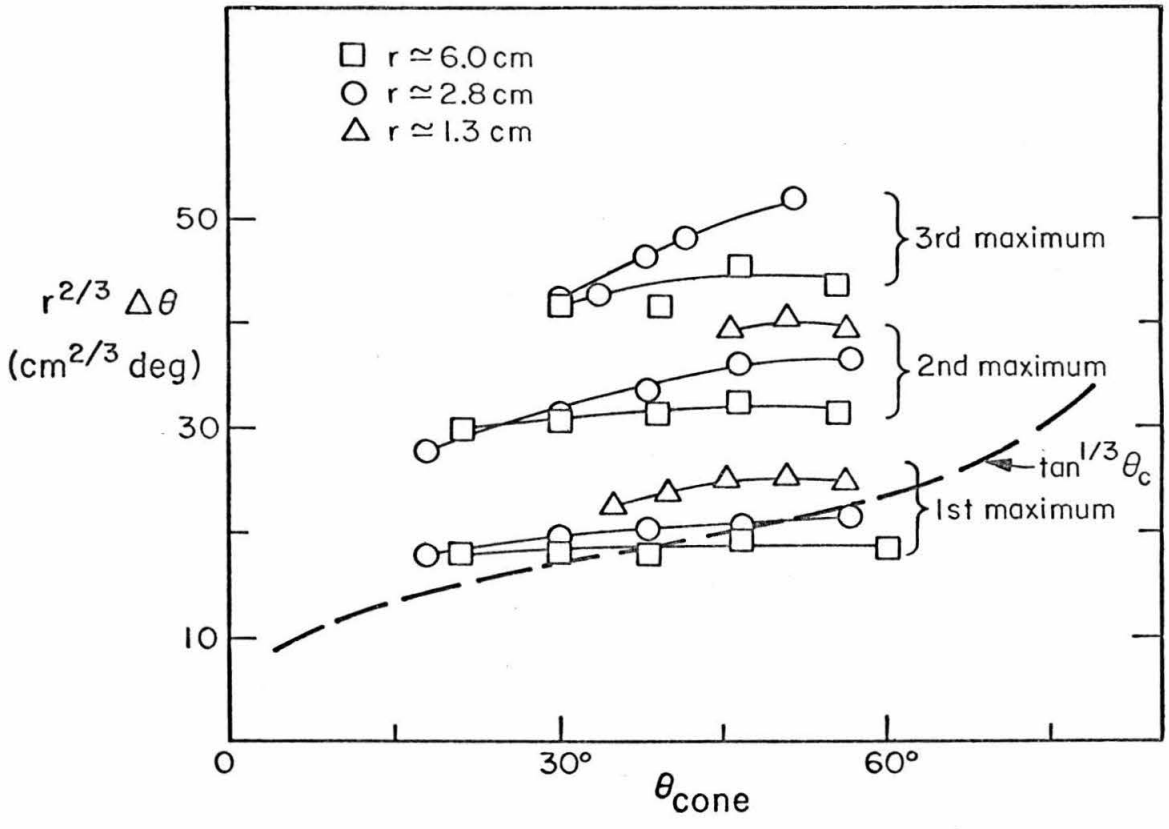

Fig. 6.4 Dependence of angular interference spacing on resonance cone angle. Vertical axis is $r^{2/3}\,\Delta\theta$ so that data taken at three different probe separations can be presented on a single plot. The dashed line is theoretical relationship $\Delta\theta \propto \tan^{1/3}\theta_c$ on an arbitrary vertical scale. Data for the measured angular spacing between the first, second and third maximum and the cone are presented.

the square points with $r \simeq 6$ cm. The horizontal axis is θ_c, the resonance cone angle. For each probe separation, data corresponding to the measured angular spacing between the first, second and third maxima of the interference structure and the cone are shown (the location of the third maximum was not measurable for $r \simeq 1.3$ cm).* For a given plasma density, electron temperature and probe separation, the angular spacing should obey $\Delta\theta \propto \tan^{1/3} \theta_c$ (see equation (6.3)). The dashed line in Fig. 6.4 is a plot of $\tan^{1/3} \theta_c$ on an arbitrary vertical scale to allow qualitative comparison of theory and experiment. The measured variation of $\Delta\theta$ with cone angle was, in general, somewhat flatter than $\tan^{1/3} \theta_c$, especially for $r \simeq 6$ cm, perhaps indicating the need for a finite magnetic field theory.

---

*The data at different probe separations were taken on different days and ω_p and v_{th} were probably different for each probe separation and were not measured. This is the reason why the curves for $r \simeq 1.3$, 2.8 and 6 cm do not fall closer together for a given maximum.

VII. CONCLUSIONS

7.1 Summary and Evaluation of Results

This thesis represents the first experimental verification of the existence of the widely discussed resonance cones. The cones were shown to exist regardless of the charge distribution on the exciting probe and the cone angle was observed to vary with incident probe frequency, cyclotron frequency, and plasma frequency in agreement with simple cold plasma dielectric theory.

Measurement of the resonance cone angle was shown to give a diagnostic measure of the plasma density in a plasma in a magnetic field. Since the theory of Langmuir probes is not completely understood in the presence of a magnetic field, and since many plasmas are too small to be reliably analyzed using a microwave interferometer, the resonance cone measurement could be a very useful diagnostic tool.

This investigation was originally undertaken in part as an experimental check on what might be observed if a satellite equipped with a transmitting and receiving probe were sent aloft into the ionosphere. Since the ionosphere is an anisotropic plasma in the presence of the earth's magnetic field, then as the satellite tumbled in space, the signal propagating between the two antennas might be expected to exhibit peaks when the line between the two antennas happened to be along the surface of one of the resonance cones set up by the transmitting antenna. If the orientation of the satellite were known with respect to the earth's magnetic field by some independent measurement, then the cone angle could be used to calculate the plasma

density in the ionosphere.

The group and phase velocities of the waves contributing to the fields were shown to be perpendicular on the resonance cones, thus clarifying the relationship of these cones to the limiting phase-velocity resonance cones which appear in the theory of plane wave propagation. It is felt that the necessity for examining the allowed directions of the group velocity and the group velocity plots, rather than the allowed directions of the phase velocity and customary phase velocity plots, when determining whether propagation between two remote points in a plasma is possible, has not been sufficiently emphasized. The term "allowed directions of propagation" has been loosely applied in the literature to mean the allowed directions of the propagation vector $\underline{k}$ rather than the directions in which the propagation of signals and information is possible, and this has led to some misleading statements and confusion.

The addition of electron thermal velocities to the theory could be easily treated only in the limit of a large static magnetic field ($\omega_c >> \omega_p, \omega$). Two important effects were observed. The resonance cone angle was shifted to a slightly smaller angle than that predicted by cold plasma theory, and an interference structure appeared inside the cones. This structure was shown to result from an interference between a fast electromagnetic wave ($v_g \sim c$) and a slow plasma wave ($v_g \sim v_{th}$). The angular interference spacing was shown to be independent of the type and orientation of the probe exciting the waves, allowing quantitative comparisons of theory and experiment to be made. The electron temperature inferred from a comparison of the experimental angular

spacing to that calculated theoretically was in agreement with an independent Langmuir probe measurement. The interference spacing was also shown to vary with the probe separation in agreement with theory.

7.2 Suggestions for Further Work

There is a definite need for a warm plasma theory which is valid for a finite magnetic field. The maximum magnetic field available in these experiments did not allow ω_c to be very large compared to ω_p and ω. This is the assumed explanation for the lack of complete agreement between experiment and theory in the measurements of the angular interference spacing as a function of cone angle described in Section 6.2. A finite magnetic field warm plasma theory would also allow an investigation of the structure of the upper branch cones. Preliminary experimental measurements indicate an interference structure which appears outside the resonance cones for the upper branch. This would be expected by analogy with the CMA diagrams; propagation is allowed inside the cones in the lower branch, and outside the cones for the upper branch. A theory valid for a finite magnetic field would also allow examination of the connection between the slow plasma waves described here and the cyclotron harmonic waves present in the experiments of Harp [36] for propagation across the magnetic field ($\theta = 90^{\circ}$).

There are many possibilities for further experimental work. The plasma wave has been observed only through its interference with the electromagnetic wave. A pulsed experiment would allow time

resolution of the total received signal into the fast electromagnetic wave ($v_g \sim c$) and the slow plasma wave ($v_g \sim v_{th}$). Some preliminary pulse measurements have proven unsuccessful with very little, if any, slow wave observable. Since the sheath around the probe should decrease the plasma wave contribution, biasing the probes to reduce the sheath might help to increase the plasma wave signal.

The desirability of having an experimental probe which produces known dipole fields has been discussed. If all the frequencies in the experiment (ω_p,ω_c, and ω) could be scaled higher by increasing the static magnetic field strength, etc., then it might be possible to construct a half-wave dipole which is still small enough to allow spatial resolution in the angular field measurements. This would allow further comparisons of experiment and theory, e.g., the amplitude of the interference structure in the field pattern, and the phase shift in passing through the resonance cone. This would also allow measurements of the impedance of the dipole as a function of the plasma parameters, a problem which has drawn considerable theoretical work in the literature.

Finally, it was noted in Section II that resonance cones should also be expected to appear at frequencies less than the ion cyclotron frequency. In the present investigation no attempt has been made to observe these cones. An experimental study of these ion branch cones might prove interesting due to the additional dependence of this resonance on the motion of the ions in the plasma as well as that of the electrons, so that information about the ions may possibly be obtained.

APPENDIX A

VOLUME 22, NUMBER 21 PHYSICAL REVIEW LETTERS 26 MAY 1969

RESONANCE CONES IN THE FIELD PATTERN OF A SHORT ANTENNA IN AN ANISOTROPIC PLASMA*

R. K. Fisher† and R. W. Gould
California Institute of Technology, Pasadena, California 91109
(Received 10 March 1969)

We report experimental observation of resonance cones in the angular distribution of the radio-frequency electric field of a short antenna in a plasma in a static magnetic field. The cone angle is observed to vary with incident frequency, cyclotron frequency, and plasma frequency in agreement with simple plasma dielectric theory. We discuss the relationship of these cones to the limiting phase- and group-velocity cones which appear in the theory of plane wave propagation.

The electromagnetic fields and radiation of a short dipole antenna in an anisotropic plasma have been the subject of many theoretical studies,[1-4] and have become of practical interest in connection with investigations employing rocket and satellite vehicles. The analysis of an oscillating point dipole shows that the fields should become infinite along a cone whose axis is parallel to the static magnetic field and whose opening angle is determined by the plasma density, magnetic field strength, and incident frequency. It has also been shown that the Poynting vector is singular along these cones, yielding an infinite radiation resistance for the point dipole antenna, a result which has stirred considerable controversy.[5] Effects such as electron collisions, electron thermal velocities, and antennas of nonzero dimensions would be expected to cause the fields to remain finite along the cones. We report here experimental verification of the existence of resonance cones along which the observed fields become very large.

Consider an antenna oscillating at frequency ω in an infinite cold plasma with an applied static magnetic field $\vec{B}_0 = B_0\hat{z}$. The near-zone fields ($r \ll c/\omega$) may be derived using the quasistatic approximation $\vec{E} = -\nabla\varphi$. We must solve Poisson's equation $\nabla\cdot\vec{D} = \rho_{\text{ext}}$, where $\vec{D} = \epsilon_0 K\cdot\vec{E}$ and K is a tensor with $K_{xx} = K_{yy} = K_\perp$, $K_{xy} = -K_{yx} = K_H$, and $K_{zz} = K_\parallel$ as its nonzero components. Neglecting terms of order m_e/m_i, we have $K_\perp = 1-\omega_p^2/(\omega^2-\omega_c^2)$ and $K_\parallel = 1-\omega_p^2/\omega^2$. Using Fourier transform methods we may solve for the potential of an oscillating monopole $\rho_{\text{ext}} = qe^{-i\omega t}\delta(\vec{r})$, yielding

$$\varphi(\rho, z) = qe^{-i\omega t}(4\pi\epsilon_0)^{-1}(K_\perp{}^2K_\parallel)^{-\frac{1}{2}} \times(\rho^2/K_\perp + z^2/K_\parallel)^{-\frac{1}{2}} \quad (1)$$

in cylindrical coordinates. To solve for the potential and fields of an oscillating dipole we merely take the appropriate derivatives. All spatial derivatives of Eq. (1) will also have a singularity along the cone defined by the vanishing of the denominator,

$$K_\parallel\sin^2\theta + K_\perp\cos^2\theta = 0, \quad (2)$$

where $\theta = \tan^{-1}\rho/z$ is the polar angle in spherical coordinates. Thus the cones exist only in the frequency regions where either $K_\parallel$ or $K_\perp$ becomes negative, but not both. In a magnetoplasma these regions are ω less than both ω_p and ω_c, hereafter called the "lower branch," and ω greater than both ω_p and ω_c but less than the upper hybrid frequency $(\omega_p^2+\omega_c^2)^{1/2}$, hereafter called the "upper branch." From Eq. (2) the resonance cone angle is given by

$$\sin^2\theta = \omega^2(\omega_p{}^2+\omega_c{}^2-\omega^2)/\omega_c{}^2\omega_p{}^2. \quad (3)$$

Kuehl[3] and others predict that the fields also become singular at these same cone angles in the far-zone region ($r \gg c/\omega$).

Using a steady-state argon rf discharge (pressure $\simeq 1\mu$) in the apparatus illustrated in Fig. 1(a), an experimental search for these cones was undertaken and proved successful. The source, or transmitting antenna, was fixed in the center of the plasma column. A second antenna was used to probe the fields set up by the transmitting antenna. This receiving antenna was constructed to rotate in a circular arc whose center is the transmitting antenna. The received signal was fed into a heterodyne receiver whose output drove an X-Y recorder. A typical trace showing the power received by the rotating probe versus the angle the rotating probe makes with the magnetic field direction is also included in Fig. 1(b). When the cone angle exceeded about 60°, multiple re-

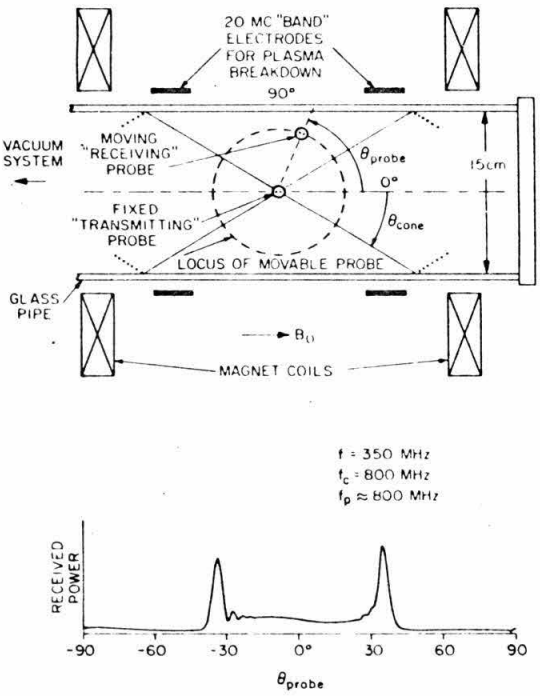

FIG. 1. (a) Schematic of experiment to measure resonance cone angles. (b) Portion of a typical trace showing the power received by the moving probe versus the angle the receiving probe makes with the magnetic field direction.

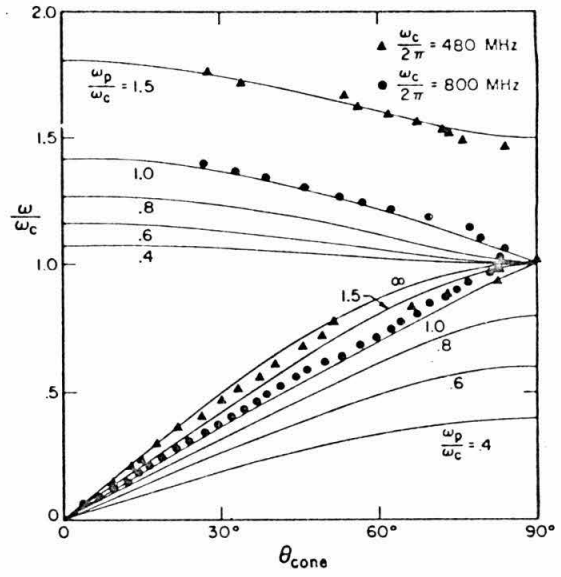

FIG. 2. Graph showing the experimentally observed location of the resonance cone angle versus the ratio ω/ω_c. Solid curves are those predicted by Eq. (3) for labeled values of ω_p/ω_c.

flections from the glass walls [dashed lines in Fig. 1(a)] complicated the traces.

The plasma density and magnetic field were held constant and traces were taken at various incident frequencies. Figure 2 is a plot of the experimentally observed cone angle versus the ratio ω/ω_c for two different values of ω_c. On the same graph the cone-angle–frequency relationship predicted by Eq. (3) is plotted for various values of the parameter ω_p/ω_c. The two sets of experimental data indicate a density roughly corresponding to $\omega_p/\omega_c \simeq 1$ and 1.5 (or $n_e \simeq 8\times10^9$ cm^{-3} and 6.5×10^9 cm^{-3}, respectively). An independent measurement using a 10.5-GHz microwave interferometer (not shown in Fig. 1) confirms these electron densities to within 20%. Data taken at the lower magnetic field show the upper and lower branches clearly separated by a frequency band in which, as predicted, no cones were present.

The cones studied in this experiment, which we shall refer to as group-velocity cones since they describe directions in which the group velocity vanishes, occur at the complementary angle of the phase-velocity cones which arise in the theory of plane-wave propagation.[6] The latter are sometimes referred to as resonance cones because the index of refraction tends to infinity (and the phase velocity tends to zero) as the angle ψ between the wave vector and the static magnetic field tends to the (phase-velocity) cone angle ψ_C. The latter are just the limiting cones in the Clemmow-Mullaly-Allis diagrams[6] which indicate the allowed direction (with respect to the magnetic field) and magnitude of the phase-velocity vectors. For the lower branch the angle ψ must be less than ψ_C, and for the upper branch the angle ψ must be greater than ψ_C. Kuehl,[3] in discussing the fields of an oscillating dipole in an uniaxial plasma ($B_0 \to \infty$, for which there is no upper branch), shows that Poynting vector is nonzero only inside the group-velocity cone. Now in an anisotropic plasma the directions of the phase velocity and group velocity are generally different. Indeed, for the uniaxial case where cones exist ($\omega^2 < \omega_p^2$), we have shown that as the angle ψ of the phase-velocity vector increases from 0 to ψ_C, the angle θ of the group-velocity vector increases from 0 to $\theta_C = \frac{1}{2}\pi - \psi_C$, the complementa-

ry angle. Although the group velocity tends to zero as $\theta \to \theta_c$, the Poynting vector and energy density tend to infinity.[3] We believe that the necessity for examining allowed directions of the group-velocity vector rather than the allowed directions of the phase-velocity vector, when determining whether transmission between two antennas in a plasma in a magnetic field is possible, has not been sufficiently emphasized. While our experiment was not performed in the far-field region, the observed cone angles are those predicted by considerations of the group velocity and the fields in the far zone.

Measurement of the resonant cone angle can also be used as a diagnostic measure of the plasma density in a plasma in a magnetic field. The upper branch especially is very dependent on the electron density. This experiment was originally undertaken in part as an experimental check on what might be observed when a satellite equipped with a transmitting and a receiving antenna is sent aloft into the ionosphere. Since the ionosphere is an anisotropic plasma in the presence of the earth's magnetic field, then as the satellite tumbles in space, the signal propagating between the two antennas might be expected to exhibit peaks when the line between the antennas happens to lie along the surface of one of the cones set up by the transmitting antenna. Note that inclusion of the ion terms in the expressions for the plasma dielectric tensor would predict similar cones at frequencies near the ion cyclotron frequency.

In conclusion, we have experimentally observed the widely discussed resonance cones. We noted that similar cones might be expected to appear near the ion cyclotron frequency. We attempted to clarify the apparent discrepancy between the angle at which these cones appear and the limiting phase-velocity cones which occur in the theory of plane-wave propagation. Further studies into the nature of these cones is being undertaken.

---

*Research supported in part by the U. S. Atomic Energy Commission and in part by the Office of Naval Research.

†National Science Foundation Predoctoral Fellow.

[1]F. V. Bunkin, Zh. Eksperim. i Teor. Fiz. 32, 338 (1957) [translation: Soviet Phys.-JETP 5, 277 (1957)]; H. Kogelnik, J. Res. Natl. Bur. Std. (U.S.) 64D, 515 (1960); E. Arbel and L. B. Felsen, in Electromagnetic Theory and Antennas, edited by E. C. Jordan (Pergamon Press, New York, 1963), p. 421.

[2]B. P. Kononov, A. A. Rukhadze, and G. V. Solodukhov, Zh. Tekh. Fiz. 31, 565 (1961) [translation: Soviet Phys.-Tech. Phys. 6, 405 (1961)]. Their analysis of the near-zone fields is incorrect. The expression [in Eq. (I-3)] for the field outside the cones should be identical (i.e., nonzero) to that inside the cones.

[3]H. H. Kuehl, Phys. Fluids 5, 1095 (1962).

[4]T. R. Kaiser, Planet Space Sci. 9, 639 (1962); K. G. Balmain, IEEE Trans. Antennas Propagation AP-12, 605 (1964).

[5]H. Staras, Radio Sci. 1, 1013 (1966); K. S. H. Lee and C. H. Papas, Radio Sci. 1, 1020 (1966); D. Walsh and H. Weil, Radio Sci. 1, 1025 (1966); K. S. H. Lee and C. H. Papas, Radio Sci. 1, 1027 (1966).

[6]W. P. Allis, S. J. Buchsbaum, and A. Bers, Waves in Anisotropic Plasmas (Massachusetts Institute of Technology Press, Cambridge, Mass., 1963), Chap. 3; T. H. Stix, The Theory of Plasma Waves (McGraw-Hill Book Company, Inc., New York, 1962), Chaps. 2 and 3; G. Bekefi, Radiation Processes in Plasmas (John Wiley & Sons, Inc., New York, 1966), Chap. 1.

APPENDIX B

VALIDITY OF QUASI-STATIC SOLUTION

The validity of the quasi-static solutions presented in Sections II and VI is not simply that the near-zone condition ($r \ll c/\omega$) apply. The following analysis is due to B. Fried [37]. At a given point $\underline{r}$ in the wave zone ($r \gg c/\omega$), the dominant contribution to $\underline{E}$ as given by a saddle point approximation is a wave (or waves) whose wave number $\underline{k}$ obeys three conditions:

(a) The dispersion equation is satisfied

$$\Delta(\underline{k},\omega) = 0 \tag{B.1}$$

where

$$\Delta = \det(\underline{\underline{\varepsilon}} + n^2\underline{\underline{1}} - \underline{n}\,\underline{n}) \quad ;$$

(b) $\underline{k}$, $\underline{r}$, and $\underline{B}_o$ lie in the same plane ;

(c) The group velocity $\underline{v}_g = d\omega/d\underline{k}$ associated with $\underline{k}$ lies along $\underline{r}$ which is equivalent to the condition

$$\tan(\theta - \psi) = \frac{\partial\Delta/\partial k}{k\partial\Delta/\partial\psi} \tag{B.2}$$

where θ and ψ are the angles which $\underline{r}$ and $\underline{k}$ make with $\underline{B}_o$. For given θ, these conditions determine k and ψ, from which the amplitude and phase of the dominant terms in $\underline{E}(\underline{r})$ can be determined.

If the parameters $(\omega,\omega_p, \omega_c,\theta)$ are such that the value of k given by equations (B.1) and (B.2) is infinite, as is possible for the cold plasma dispersion relation, then the amplitude of $\underline{E}$ is also singular. (This is not obvious, but comes out of a saddle point

calculation.) Moreover, the right side of equation (B.2) is then of order k^2, so $\theta - \psi$ must be $\pi/2$. Hence the direction of $\underline{k}$ is normal to $\underline{r}$ and, by condition (c), to the group velocity. To find the angle θ of the resonance cone, therefore, one need only find a value of ψ at which the dispersion equation gives an infinite value for $n = kc/\omega$; its complement will be θ . In the cold plasma case where

$$\Delta = A(\omega,\psi)\ n^4 - B(\omega,\psi)\ n^2 + C(\omega) \tag{B.3}$$

(Notation defined in Stix [32], pp. 10-12), n can be infinite only if $A = 0$. It is then clear why the quasi-static form of the dispersion relation

$$\Delta_{es} = \underline{k} \cdot \underline{\underline{\varepsilon}} \cdot \underline{k}/k^2 = 0 \tag{B.4}$$

gives the correct value of ψ and hence of θ , since $\Delta_{es} = \varepsilon_\perp \sin^2\theta + \varepsilon_{||} \cos^2\theta = A$. When dealing with a resonance (n infinite), electrostatic approximations are generally valid.

The quasi-static solution can be seen to be valid near the resonance cones in still another manner. Maxwell's equations allow the electric field of a source to be obtained from the vector and scalar potentials

$$\underline{E} = -\nabla\phi - \frac{1}{c}\frac{\partial \underline{A}}{\partial t} \tag{B.5}$$

In using the quasi-static approximation the contributions to the electric field due to the vector potential $\underline{A}$ are neglected. Considering a z-directed dipole in a uniaxial plasma for simplicity, the

electric field can be shown [10] to contain terms proportional to r^2/R^5, r^2/R^4 and r^2/R^3 where $r = [\rho^2 + z^2]^{1/2}$ and $R = [(\rho^2/K_\perp) + (z^2/K_{||})]^{1/2}$ which vanishes on the resonance cones. The only term which is important near the cone is the r^2/R^5 term which also arises from our quasi-static solution for the potential $\emptyset$. Thus the contributions from the vector potential are not important near the cone.

APPENDIX C

PROBE DESIGN AND CONSTRUCTION

The probes used in this experiment were constructed from .070" or .087" O.D. semi-rigid 50Ω coaxial cable (Microax UT-701 and UT-85C). Both the inner and outer conductors were chosen to be non-magnetic (copper) to prevent distortion of the static magnetic field near the probes. The radiating portion of the probes consisted of approximately 2 mm of exposed center conductor as shown in Fig. C.1.

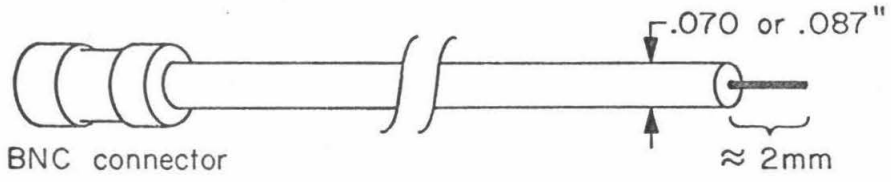

Fig. C.1. Probe construction

A portion of the probe length was enclosed and soldered inside a section of 1/4" O.D. polished brass tubing so that it could be fed through a 1/4" double O-ring rotary vacuum seal (CVC type no. SR-25). The probe was vacuum-sealed with epoxy at one end and a BNC connector attached. On some probes the portion of the outer conductor inside the plasma was covered with teflon tubing to prevent sputtering of the copper onto the glass walls of the plasma container. This had no noticeable effect on the experimental results.

The two important quantities measured in these experiments, cone angle location and angular interference spacing, are independent

of the type of probes used. It would have been desirable, however, if a dipole probe could have been constructed so that additional comparisons of theory and experiment could have been made. The probes described above did not produce simple dipole fields (see Section 4.2) and could not be easily treated theoretically. Some unsuccessful attempts were made to construct dipole probes and these are described briefly below.

The dipole probe design tried is shown in Fig. C.2. The signal was applied across (A) and (B) and it was hoped that the electric field would be that of a dipole oriented parallel to the arms of the probe.

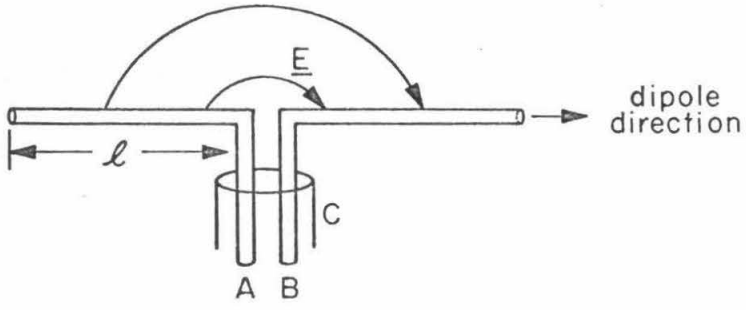

Fig. C.2. Dipole probe

At first the probe was fed using semi-rigid coax with one of the arms (B) of the probe connected to the signal generator through the outer conductor (C). This failed to produce dipole fields and the cause was felt to be the unbalanced nature of the probes. New probes were built with the signals on arms (A) and (B) made symmetric with respect to the outer conductor (C) through use of a balanced transformer between the signal generator and the probe. These probes produced fields that seemed to be dipole in nature but only at distances less than or equal

to a few times the length of the probes ($2\ell \simeq 2.5$ cm), and thus were not practical for making experimental measurements, since the transmitting and receiving probes must be small compared to the probe separation to insure the angular resolution needed in the experiment.

APPENDIX D

SOLUTION FOR POTENTIAL OF OSCILLATING CHARGE IN WARM UNIAXIAL PLASMA BY METHOD OF STATIONARY PHASE

The following analysis is due to R. Gould [38]. In Section VI, equation (6.2) the potential of an oscillating charge in a warm uniaxial plasma ($2kT_e = mv_{th}^2$, $B_o = \infty$) was found to be

$$\phi(\rho,z) = \frac{qe^{-i\omega t}}{4\pi^2 \varepsilon_o} \int_{-\infty}^{\infty} K_o(k_{||} \rho \sqrt{K_{||}}) \, e^{ik_{||} z} \, dk_{||} \tag{D.1}$$

where

$$K_{||} = 1 - \frac{\omega_p^2}{k_{||}^2 v_{th}^2} Z'\left(\frac{\omega}{k_{||} v_{th}}\right) \tag{D.2}$$

Near the resonance cone we can use the large argument expansion for the modified Bessel function

$$K_o(k_{||} \rho \sqrt{K_{||}}) \simeq \sqrt{\frac{\pi}{2k_{||} \rho \sqrt{K_{||}}}} \, e^{-k_{||} \rho \sqrt{K_{||}}} \tag{D.3}$$

so that equation (D.1) becomes

$$\phi(\rho,z) = \frac{qe^{-i\omega t}}{4\pi^2 \varepsilon_o} \int_{-\infty}^{\infty} \sqrt{\frac{\pi}{2k \rho \sqrt{K_{||}}}} \, e^{ik_{||} z - k_{||} \rho \sqrt{K_{||}}} \, dk_{||} \tag{D.4}$$

which can be written

$$\phi(\rho,z) = \int_{-\infty}^{\infty} A(k_{||}) \, e^{i\Phi(k_{||})} \, dk_{||} \tag{D.5}$$

where

$$\Phi(k_{||}) = k_{||} z + ik_{||} \rho \sqrt{K_{||}} \tag{D.6}$$

We can approximately evaluate integral (D.5) using the method of stationary phase. Because of the rapidly oscillating character of $\exp[i\Phi(k_{\parallel})]$, the contributions to the integral from the neighborhood of $k_{\parallel}$ will largely cancel unless

$$\Phi'(k_{\parallel}) = z + i\rho\sqrt{K_{\parallel}} + ik_{\parallel}\rho\, K_{\parallel}'/\sqrt{K_{\parallel}} = 0 \tag{D.7}$$

Expanding $\Phi(k_{\parallel})$ in a Taylor series about $k_{\parallel o}$, a root of equation (D.7)

$$\Phi(k_{\parallel}) \simeq \Phi(k_{\parallel o}) + \frac{1}{2}\Phi''(k_{\parallel o})\,(k_{\parallel} - k_{\parallel o})^2 \tag{D.8}$$

and using the result

$$\int_{-\infty}^{\infty} e^{i\alpha u^2}\, du = \frac{\pi}{\alpha}\, e^{i(\pi/4)} \tag{D.9}$$

we find that

$$\phi(\rho,z) \propto e^{i\Phi(k_{\parallel o})} \tag{D.10}$$

which we will use to find the angular interference spacing.

First we must find the roots of (D.7). For low temperatures $(k_{\parallel} v_{th} << \omega)$

$$K_{\parallel} \simeq 1 - \frac{\omega_p^2}{\omega^2}\left(1 + \frac{3k_{\parallel}^2 v_{th}^2}{2\omega^2}\right) \equiv -\alpha^2\left(1 + \frac{3\omega_p^2 k_{\parallel}^2 v_{th}^2}{2\alpha^2\omega^4}\right) \tag{D.11}$$

where $\alpha^2 = \omega_p^2/\omega^2 - 1 > 0$ in the frequency region where cones will exist. Thus

$$K_{\parallel}' = -\frac{3\omega_p^2}{\omega^4} k_{\parallel} v_{th}^2 \tag{D.12}$$

Substituting (D.11) and (D.12) into (D.7), we obtain

$$\Phi'(k_{\parallel}) \simeq z - \alpha\rho \left(1 + \frac{9}{4}\frac{\omega_p^2 k_{\parallel}^2 v_{th}^2}{\alpha^2 \omega^4}\right) \text{ for } \frac{2k_{\parallel}^2 v_{th}^2}{3\omega^2} << 1 - \frac{\omega^2}{\omega_p^2} \quad \text{(D.13)}$$

Let $\eta \equiv z - \alpha\rho > 0$ so that we are inside the resonance cone. Then $\Phi'(k_{\parallel}) = 0$ when

$$\frac{\omega_p^2 k_{\parallel_o}^2 v_{th}^2}{\alpha^2 \omega^4} = \frac{4}{9}\frac{\eta}{\alpha\rho} \quad \text{(D.14)}$$

Substituting (D.14) and (D.11) into (D.6) and simplifying, remembering the condition in (D.13) on v_{th}, we obtain

$$\Phi(k_{\parallel_o}) \simeq \frac{\omega^2 \rho \alpha^2}{\omega_p v_{th}} \left(\frac{4\eta}{9\alpha\rho}\right)^{3/2} \quad \text{(D.15)}$$

Using $\sin\theta_c = \omega/\omega_p$, we can show that

$$\alpha = \left(\frac{\omega_p^2}{\omega^2} - 1\right)^{1/2} = \cot\theta_c \quad \text{(D.16)}$$

and

$$\eta = z - \alpha\rho = \frac{r}{\sin\theta_c}\sin(\theta_c - \theta) \simeq \frac{r}{\sin\theta_c}(\theta_c - \theta) \quad \text{(D.17)}$$

Substituting (D.16) and (D.17) into (D.15), we find

$$\Phi(k_{\parallel_o}) \propto \frac{\omega_p r}{v_{th}}\left(\frac{\cot\theta_c}{\sin\theta}\right)^{1/2}(\theta_c - \theta)^{3/2} \quad \text{(D.18)}$$

The potential and fields are proportional to $\exp[i\Phi(k_{\parallel_o})]$ so that from equation (D.18) we find that the angular interference spacing

$$\Delta\theta \propto \left(\frac{v_{th}}{\omega_p r}\right)^{2/3} \left(\frac{\sin\theta}{\cos\theta_c}\right)^{1/3} \tag{D.19}$$

which is the desired result.

Appendix E

(from Proc. of the 9th Int. Conf. on Ionization Phenomena in Gases, Bucharest, Romania, 1969)

PANEL 4.3.1 GENERAL THEORY OF PLASMA WAVES

4.3.1.5

PHASE AND GROUP VELOCITY IN AN ANISOTROPIC PLASMA

R. W. Gould and R. K. Fisher
California Institute of Technology, Pasadena, California, U.S.A.

I. Introduction

We discuss the relationship between phase and group velocities of electromagnetic waves in a magnetoplasma. In general, they are not parallel and when the index of refraction exhibits a resonance ($n = c/v_p \to \infty$) they are nearly perpendicular. When determining whether propagation between two remote points is possible, the allowed directions of the group velocity vector are important and the usual phase velocity[1] plots are misleading.

II. Phase Velocity

We first outline the dispersion of plane harmonic waves (wave fields $\exp[i(\underline{k}\cdot\underline{r}-\omega t)]$) in a plasma in a magnetic field $\underline{B}_o = B_o \underline{e}_z$ in the z direction. Maxwell's curl equations are $\underline{k}\times\underline{E} = \omega\underline{B}$ and $\underline{k}\times\underline{B} = -(\omega/c^2)\,\underline{K}\cdot\underline{E}$ where $\underline{K} = K(\omega,\underline{k})$ is the tensor dielectric function of the plasma. For simplicity we limit our discussion to sufficiently large static magnetic fields so that, effectively, electrons move along field lines, i.e.,

$$\underline{K} = \begin{pmatrix} 1 & 0 & 0 \\ 0 & 1 & 0 \\ 0 & 0 & K \end{pmatrix} \tag{1}$$

where $K = K(\omega,k_z) = 1 + \chi(\omega,k_z)$ and χ is the susceptibility. For a cold collisionless plasma $\chi = -\omega_p^2/\omega^2$ where $\omega_p = (ne^2/\varepsilon_o m)^{1/2}$ is the plasma frequency.

For plane waves whose wave vector (and hence phase velocity) makes an angle ϕ with respect to the magnetic field, $\underline{n} = \underline{k}c/\omega = (n\sin\phi, 0, n\cos\phi)$ and the (dispersion) equation for the index of refraction n is readily found to be (with $u = \cos\phi$),

$$1 - n^2 + \chi - \chi n^2 u^2 = 0 \tag{2}$$

The solution of this equation is

$$n^2 = (c/v_p)^2 = (1+\chi)/(1+\chi u^2) \tag{3}$$

When $\omega_p^2/\omega^2 = -\chi < 1$, n is real for all angles ϕ, but when $\omega_p^2/\omega^2 = -\chi > 1$, $n^2 \to \infty$ (resonance) for $u^2 = u_c^2 = -1/\chi$ i.e., when $\cos\phi = \cos\phi_c = \omega/\omega_p$. Furthermore, when $u > u_c$, i.e., $\phi < \phi_c$, n is real (propagating waves) whereas when $u < u_c$, i.e., $\phi > \phi_c$, n is imaginary (evanescent waves). This behavior is illustrated in the right half of Fig. 1, which is a polar plot of $v_p/c = 1/n$ for $\omega_p/\omega = 2$ or $\phi_c = 60^\circ$ (the dots correspond to 5° increments in ϕ). The angle ϕ_c defines a cone, whose axis coincides with the magnetic field, within which the phase velocity vector must lie and on which it tends to zero. We refer to this as the phase velocity cone[2].

III. Group Velocity

For each $(\omega,\underline{k})$ we can associate a group velocity given by $v_g = \nabla_k[\omega(\underline{k})]$. Using 2) we can readily obtain expressions for the magnitude of the group velocity and the angle θ which it makes with the magnetic field

$$(v_g/c)^2 = \frac{(1+\chi)(1+\chi u^2)}{(1+2\chi u^2+\chi^2 u^2)} \tag{4}$$

$$\tan\theta = -\tan\phi/(1+\chi) \tag{5}$$

Thus the group velocity is not in the same direction as the phase velocity. In fact the component of v_g perpendicular to $\underline{B}_o$ is opposite to the perpendicular component of v_p. Near resonance ($n^2 \to \infty$) v_g and v_p are perpendicular (and coplanar with $\underline{B}_o$). This behavior is illustrated in the left half of Fig. 1, which is a polar plot of v_g/c. Each dot on the group velocity plot is to be associated with the corresponding dot on the phase velocity plot (e.g., A,B,C,$\cdots$). Equation (5) shows that θ increases monotonically with ϕ and reaches its maximum value θ_c at resonance ($\phi = \phi_c$). Furthermore $\psi_c + \theta_c = 90^\circ$. Thus θ_c defines a second cone, within which the group velocity vector must lie and on which it tends to zero. We refer to this cone as the group velocity cone[2]. Since propagation between two remote points is determined by the group velocity, we wish to emphasize the importance of v_g and hence the group velocity cone rather than the customary phase velocity plots and cone.

For the case studied here ($B_o \to \infty$) ϕ_c decreases from 90° to 0°, whereas θ_c increases from 0° to 90° when ω/ω_p increases from 0 to 1. When $\omega/\omega_p > 1$ the cones do not exist.

IV. Effect of Electron Thermal Velocities

The behavior near resonance is modified substantially by the inclusion of electron thermal velocities, since $\chi = -\omega_p^2/(\omega^2 - k_z^2v^2)$ with $v^2 = 3kT_e/m \equiv 3\delta^2c^2$. Equation (2) becomes

$$n^4(u_c^2u^2\delta^2) + n^2(u^2 - u_c^2 - u_c^2u^2\delta^2) - (1-u_c^2) = 0 \tag{6}$$

When $n^2 \ll 1/\delta^2$, Eq. (3) is recovered, and when $n^2 \gg 1/\delta^2$

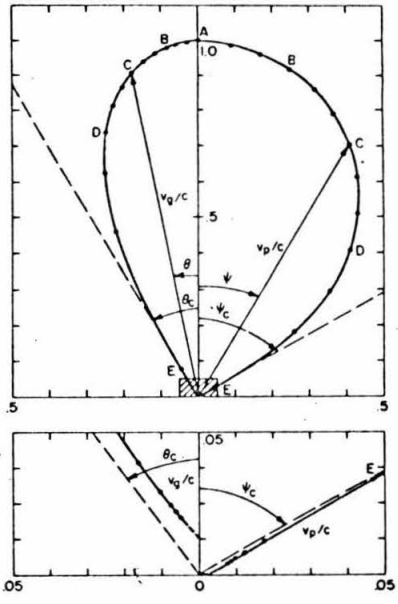

Figure 1. Polar plot of phase velocity (right side) and group velocity (left side) for $B_o \to \infty$, $\omega_p/\omega = 2$. Lower plot shows shaded region, where electron thermal velocities are important, on an expanded scale.

$$n^2 = \frac{u^2 - u_c^2}{u_c^2u^2\delta^2} \tag{7}$$

The modification in the polar phase and group velocity plots are shown in the lower part of Fig. 1 for $\delta = .01$. (Dots correspond to 1° increments). We see that inclusion of electron thermal velocity effects now permits all values of ϕ but θ is nevertheless restricted to $\theta < \theta_c$ as before. We note also that the v_p is a single valued function of ϕ although v_g is a double-valued function of θ (one fast wave $v_g \sim c$ and one slow wave $v_g \sim \delta c$). It should also be noted that when χ is determined from the Vlasov equation, the slow waves exhibit strong Landau damping in the dashed part of Fig. 1.

V. Conclusion

By considering a special case ($B_o \to \infty$) we conclude that in an anisotropic magnetoplasma the phase and group velocities are, in general, in different directions and that the allowed directions of these two vectors are contained within two different cones, the phase velocity cone ($\phi < \phi_c$) and the group velocity cone ($\theta < \theta_c$), on which $v_p \to 0$ and $v_g \to 0$. The cone angles are complementary, i.e., $\phi_c + \theta_c = 90^\circ$. While the phase velocity diagrams are most frequently discussed, the group velocity diagrams are relevant when determining whether transmission between two spatially separated points is possible. This is further confirmed by the fact that the time average Poynting vector of a dipole antenna vanishes outside of the group velocity cone[3].

This research was sponsored by the United States Office of Naval Research.

References

1. W. P. Allis, S. J. Buchsbaum, and A. Bers, Waves in Anisotropic Plasmas, (M.I.T. Press, Cambridge, Massachusetts 1963), Chap. 3.
2. R. K. Fisher and R. W. Gould, Phys. Rev. Letters (to appear).
3. H. Kuehl, Phys. Fluids 5, 1095 (1962).

REFERENCES

[1] Bunkin, F. V., "On Radiation in Anisotropic Media", Soviet Phys. JETP 5, 277-283 (1957).

[2] Kogelnik, H., "The Radiation Resistance of an Elementary Dipole in Anisotropic Plasmas", Fourth Int. Conf. on Ioniz. Phenomena in Gases, Uppsala, IIIC, North Holland Publishing Company (1960), pp. 721-725.

[3] Kogelnik, H., "On Electromagnetic Radiation in Magneto-Ionic Media", J. Res. Natl. Bur. Stds. (U.S.) 64D, 515-523 (1960).

[4] Kuehl, H. H., "Radiation from an Electric Dipole in an Anisotropic Cold Plasma", Antenna Laboratory Report No. 24, California Institute of Technology, Pasadena, California (1960).

[5] Kuehl, H. H., "Electromagnetic Radiation from an Electric Dipole in a Cold Anisotropic Plasma", Phys. Fluids 5, 1094-1103 (1962).

[6] Kaiser, T. R., "The Admittance of an Electric Dipole in a Magneto-Ionic Environment", Planet Space Sci. 9, 639-657 (1962).

[7] Arbel, E. and Felsen, L. B., "Theory of Radiation from Sources in Anisotropic Media, Part I: General Sources in Stratified Media", Jordan, E.C., Editor, Proc. Symp. on Electromagnetic Theory and Antennas, Pergamon Press, Inc., New York (1963), pp. 391-420.

[8] Arbel, E. and Felsen, L. B., "Theory of Radiation from Sources in Anisotropic Media, Part II: Point Sources in Infinite, Homogeneous Medium", Jordan, E.C., Editor, Proc. Symp. on Electromagnetic Theory and Antennas, Pergamon Press, Inc., New York (1963), pp. 421-459.

[9] Clemmow, P. C., "On the Theory of Radiation from a Source in a Magneto-Ionic Medium", Jordan, E.C., Editor, Proc. Symp. on Electromagnetic Theory and Antennas, Pergamon Press, Inc., New York (1963), pp. 461-475.

[10] Clemmow, P. C., "The Theory of Electromagnetic Waves in a Simple Anisotropic Medium", Proc. I.E.E. 110, 101-106 (1963).

[11] Kogelnik, H. and Motz, H., "Electromagnetic Radiation from Sources Embedded in an Infinite Anisotropic Medium and the Significance of the Poynting Vector", Jordan, E.C., Editor, Proc. Symp. on Electromagnetic Theory and Antennas, Pergamon Press, Inc., New York (1963), pp. 477-493.

[12] Mittra, R. and Deschamps, G. A., "Field Solutions for a Dipole in an Anisotropic Medium", Jordan, E.C., Editor, Proc. Symp. on Electromagnetic Theory and Antennas, Pergamon Press, Inc., New York (1963), pp. 495-512.

[13] Lee, K.S.H. and Papas, C. H., "Irreversible Power and Radiation Resistance of Antennas in Anisotropic Ionized Gases", J. Res. Natl. Bur. Stds. (U.S.) 69D, 1313-1320 (1965).

[14] Staras, H., "The 'Infinity Catastrophe' Associated with Radiation in Magneto-Ionic Media", Radio Science 1, 1013-1020 (1966).

[15] Walsh, D. and Weil, H., "Irreversible Power and Radiation Resistance of Antennas in Magnetoionic Media", Radio Science 1, 1025-1027 (1966).

[16] Lee, K.S.H. and Papas, C. H., "A Further Explanation of the New Theory of Antenna Radiation with Particular Reference to Uniaxial Media", Radio Science 1, 1020-1023 (1966).

[17] Lee, K.S.H. and Papas, C. H., "On Walsh and Weil's Defense of the Conventional Method", Radio Science 1, 1027 (1966).

[18] Staras, H., "The Impedance of an Electric Dipole in a Magneto-Ionic Medium", IEEE Trans. Ant. Prop. AP-12, 695-702 (1964).

[19] Singh, N. and Gould, R.W., "Temperature Effects on the Radiation from a Short Dipole in a Uniaxial Plasma", Bull. Am. Phys. Soc. 14, 1004 (1969).

[20] Deschamps, G. and Kesler, O., "Radiation of an Antenna in a Compressible Magnetoplasma", Radio Science 2, 757-767 (1967).

[21] Tunaley, J. and Grard, R., "The Impedance of a Probe in a Warm Plasma", Ann. Geophysics (France) 25, 55-65 (1969).

[22] Lee, S. W. and Mittra, R., "Transient Radiation of an Electric Dipole in a Uniaxially Anisotropic Plasma", Radio Science 2, 813-820 (1967).

[23] Kenney, J., Electric Dipole Radiation in Isotropic and Uniaxial Plasmas, Antenna Laboratory Report No. 44, California Institute of Technology, Pasadena, California (1968).

[24] Kononov, B., Rukhadze, A.A., and Solodukhov, G.V., "Electric Field of a Radiator in a Plasma in an External Magnetic Field", Zh. Tekh. Fiz. 31, 565-573 (1961) [translation: Soviet Phys. Tech. Phys. 6, 405-410 (1961)].

[25] Balmain, K., "The Impedance of a Short Dipole Antenna in a Magnetoplasma", IEEE Trans. Ant. Prop. AP-12, 605-617 (1964).

[26] Wang, T.C.N. and Bell, T.F., "Radiation Resistance of a Short Dipole Immersed in a Cold Magnetoionic Medium", Radio Science 4, 167-177 (1969).

[27] Crawford, F.W., "A Review of Cyclotron Harmonic Phenomena in Plasmas", Nuclear Fusion 5, 73-84 (1965); Harp, R.S., "Propagation of Longitudinal Plasma Oscillations near Cyclotron Harmonics", Appl. Phys. Letters 6, 51-53 (1965).

[28] Heald, M.A. and Wharton, C.B., Plasma Diagnostics with Microwaves (John Wiley & Sons, Inc., New York, N.Y., 1965), pp. 278-280.

[29] Akhiezer, A. I., Akhiezer, I. A., Polovin, R. V., Sitenko, A.G. and Stepanov, K.N., Collective Oscillations in a Plasma, translated by H.S.H. Massey, M.I.T. Press, Cambridge, Mass., 1967; pp. 35-37.

[30] Heald, M.A. and Wharton, C.B., Plasma Diagnostics with Microwaves (John Wiley & Sons, Inc., New York, N.Y., 1965), pp. 117-123.

[31] Singh, N. and Gould, R.W. , to be published.

[32] Allis, W.P., Buchsbaum, S. J. and Bers, A., Waves in Anisotropic Plasmas , M.I.T. Press, Cambridge, Mass. (1963), Chap. 3; Stix, T.H., The Theory of Plasma Waves, McGraw-Hill, Inc., New York, N.Y., 1962, Chaps. 2 and 3; Bekefi, G., Radiation Processes in Plasmas, John Wiley & Sons, Inc., New York, N.Y., 1966, Chap. 1.

[33] Fisher, R. K. and Gould, R. W., "Resonance Cones in the Field Pattern of a Short Antenna in an Anisotropic Plasma", Phys. Rev. Letters 22, 1093-1095 (1969) [See Appendix A].

[34] Fried, B.D. and Conte, S.D., The Plasma Dispersion Function, Academic Press, New York, N.Y. (1961).

[35] Seshadri, S.R., "Effect of Insulation on the Radiation Resistance of an Electric Dipole in a Simple Anisotropic Medium, Proc. IEEE 113, 593-600 (1966).

[36] Harp, R.S., "The Dispersion Characteristics of Longitudinal Plasma Oscillations near Cyclotron Harmonics", Proc. Seventh Int. Conf. on Phenomena in Ionized Gases, II, Belgrade, Yugoslavia, pp. 294-302.

[37] Fried, B., UCLA Physics Department, private communication.

[38] Gould, R. W., California Institute of Technology, private communication.